Multilayer simulation of wind-forced breaking wave fields statistics and Langmuir turbulence

Rui Yang[1], Jiarong Wu[1,2], Nicolò Scapin[1,6], J. Thomas Farrar[3], Bertrand Chapron[4], Stéphane Popinet[5] and Luc Deike[1,6,*]

International Ocean Vector Winds Science Team (IOVWST) Meeting
Darmstadt, Germany (May, 5-8th 2025)

1. Mechanical and Aerospace Engineering, Princeton University, Princeton, NJ 08540, USA
2. Courant Institute of Mathematical Sciences, New York University, New York, NY, USA
3. Woods Hole Oceanographic Institution (WHOI), Woods Hole, MA, USA
4. IFREMER, Univ. Brest, CNRS, IRD, Laboratoire d'Océanographie Physique et Spatiale (LOPS), Plouzané, France
5. Sorbonne Universite, CNRS, Institut Jean Le Rond d'Alembert, F-75005 Paris, France
6. High Meadows Environmental Institute, Princeton University, Princeton, NJ, 08540, USA

Wave breaking - from single breakers to broadband wave field

Broadband wave field

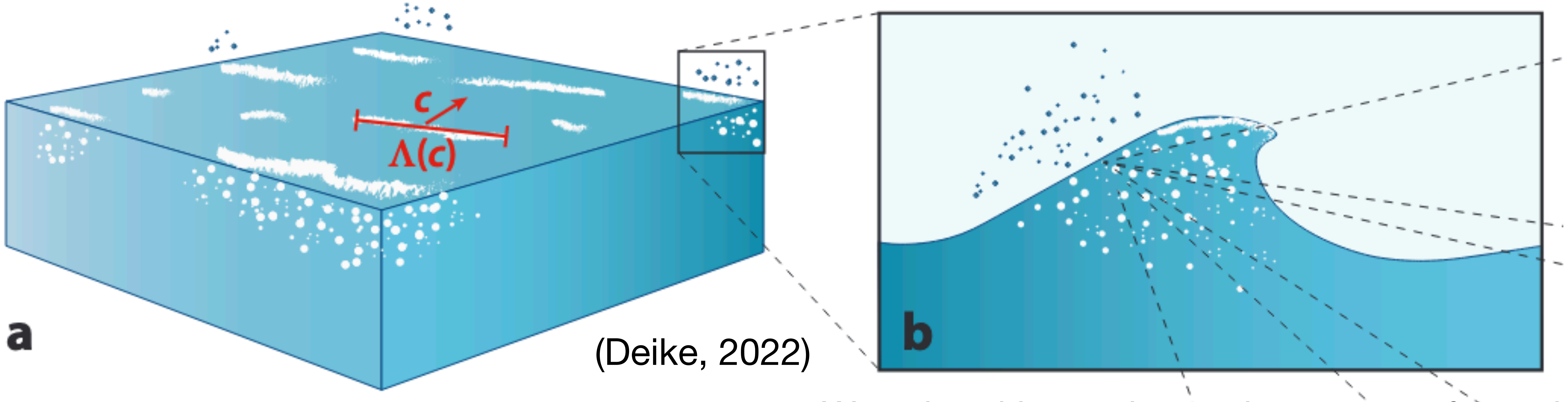

(Deike, 2022)

Single breaker

Continuous wave breaking on various scales

Wave breaking: enhanced mass transfer and contribute to upper ocean current and mixing.

Broadband wave field

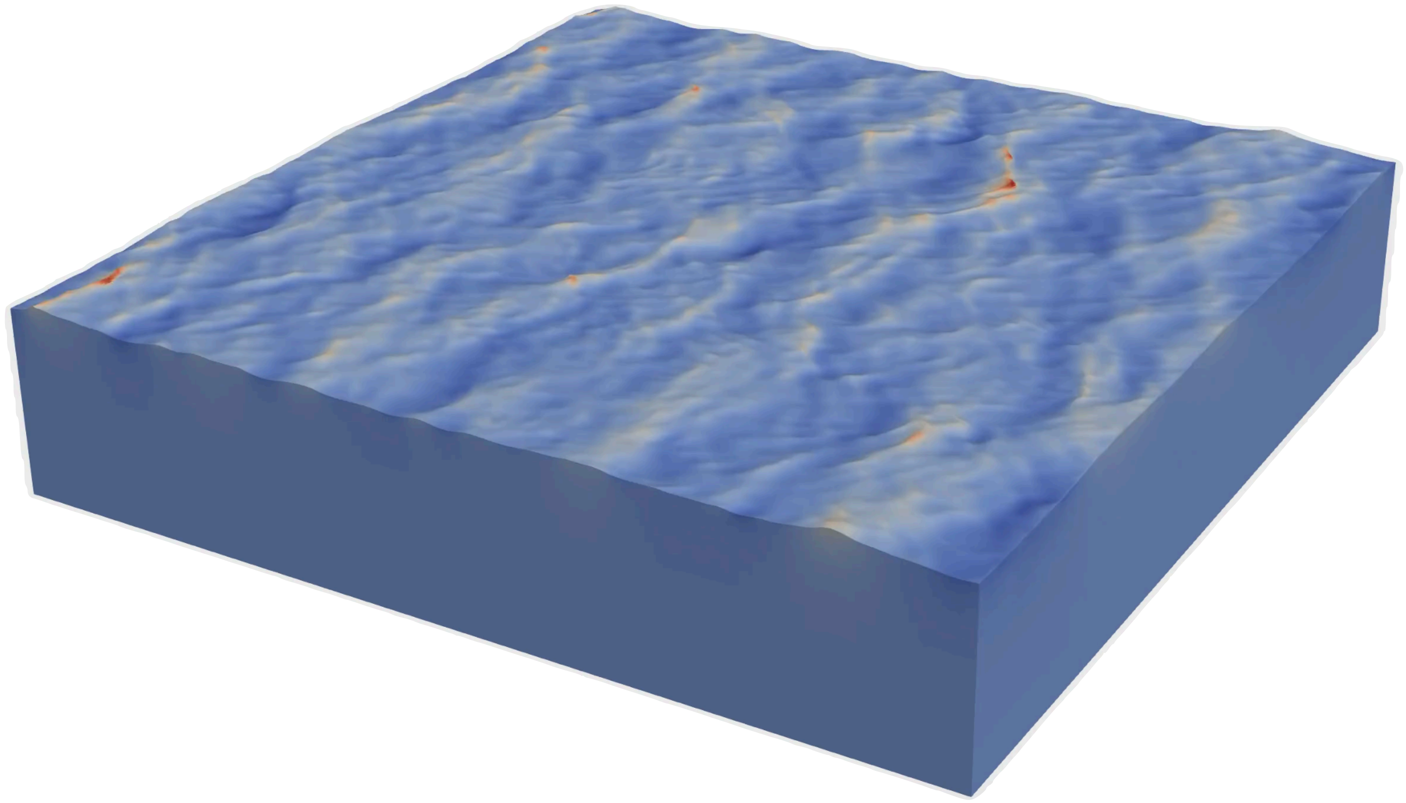

(Wu et al. 2023, 2025)

Single breaker

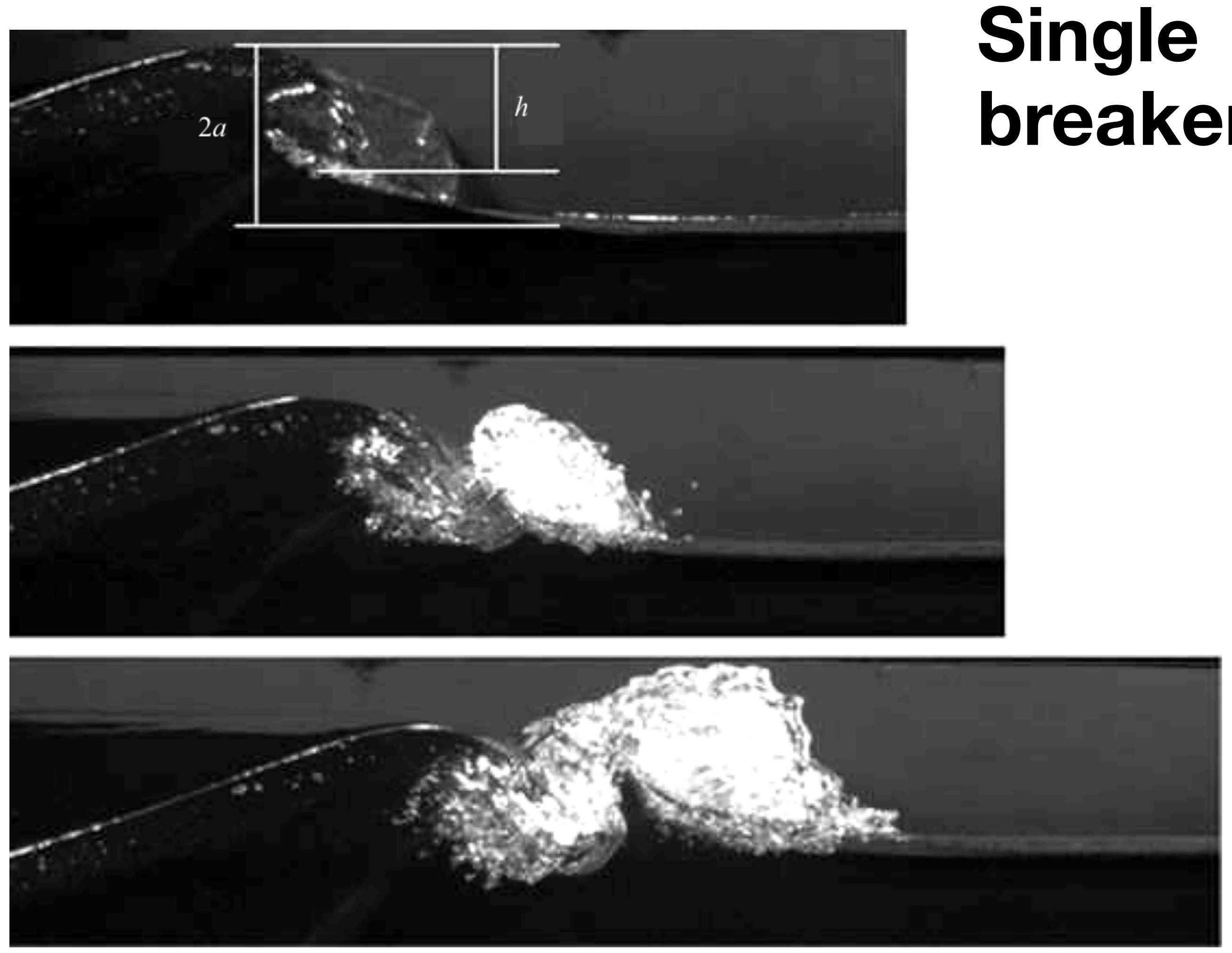

(Drazen et al. 2008)

(Mostert et al. 2022)

Goal:

- Study breaking waves statistics and underwater dissipation in the wind-forced broadband wave field.

Langmuir circulation

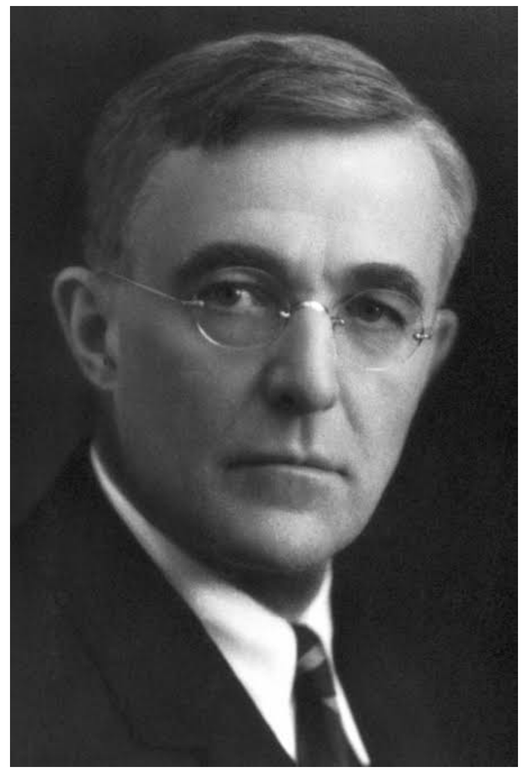

Irving Langmuir

Counter-rotating vortices near the ocean's surface and aligned with the wind, developed when wind blows steadily over the sea surface.

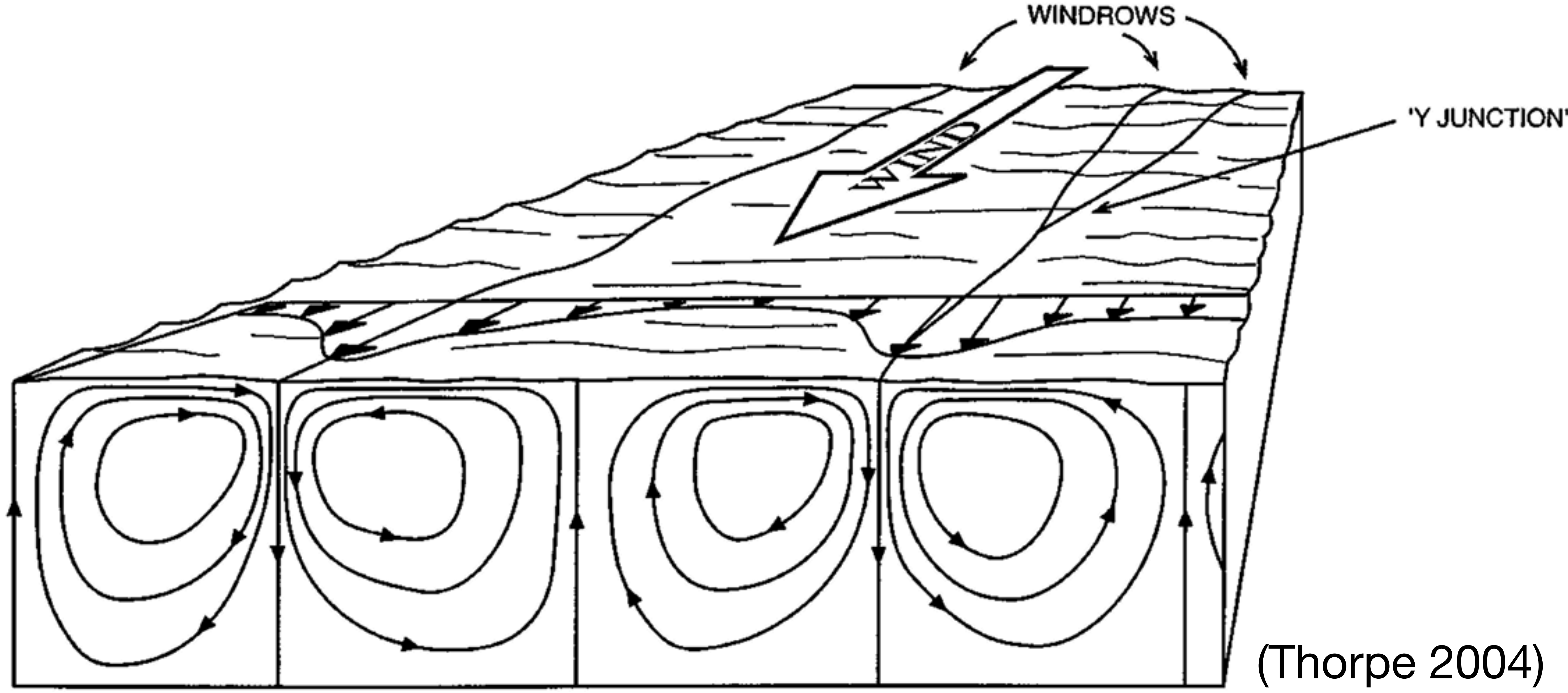

(Thorpe 2004)

- Enhances vertical and lateral ocean surface mixing
- Accelerates the dispersion of pollutants and microplastics
- Regulates the transport of surface heat, momentum, and gases

Goal:

- Study breaking waves statistics and underwater dissipation in the wind-forced broadband wave field.
- Can we observe the Langmuir circulation in simulations?

Multilayer model

Discretization structure illustration

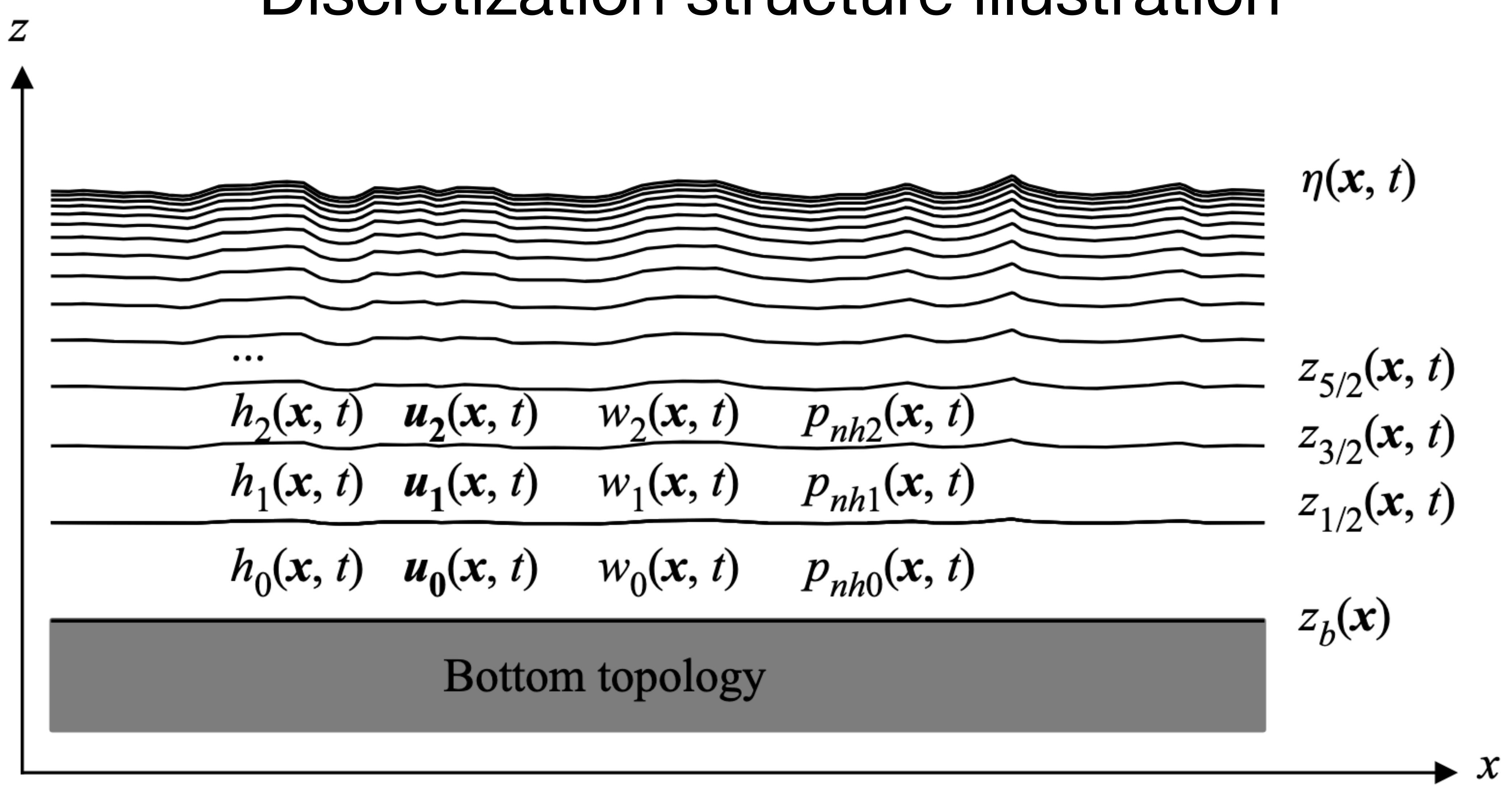

(Wu et al. 2023)

Governing equations

Layer evolution: $$\frac{\partial h_l}{\partial t} + \nabla_H \cdot (h\boldsymbol{u})_l = 0,$$

Horizontal momentum: $$\frac{\partial (h\boldsymbol{u})_l}{\partial t} + \nabla_H \cdot (h\boldsymbol{u}\boldsymbol{u})_l = -g h_l \nabla_H \eta - \nabla_H (h p_{nh})_l + [p_{nh}\nabla_H z]_l + [\nu \partial_z \boldsymbol{u}]_l + \nu \nabla_H^2 \boldsymbol{u},$$

Vertical momentum: $$\frac{\partial (hw)_l}{\partial t} + \nabla_H \cdot (hw\boldsymbol{u})_l = -[p_{nh}]_l + [\nu \partial_z w]_l + \nu \nabla_H^2 w,$$

Mass conservation: $$\nabla_H \cdot (h\boldsymbol{u})_l + [w - \boldsymbol{u} \cdot \nabla_H z]_l = 0,$$

Scalar transportation: $$\frac{\partial (hT)_l}{\partial t} + \nabla \cdot (hT\boldsymbol{u})_l = 0,$$

p_{nh}: non-hydrostatic pressure

T: passive tracer

- Multilayer model http://basilisk.fr/src/layered/README (Popinet 2020).
- Discretization: horizontally Eulerian and vertically Lagrangian coordinates.
- Bridge between the hydrostatic Saint-Venant/shallow-water equations and the incompressible Navier-Stokes equations with the interface.

Ability to simulate breaking wave

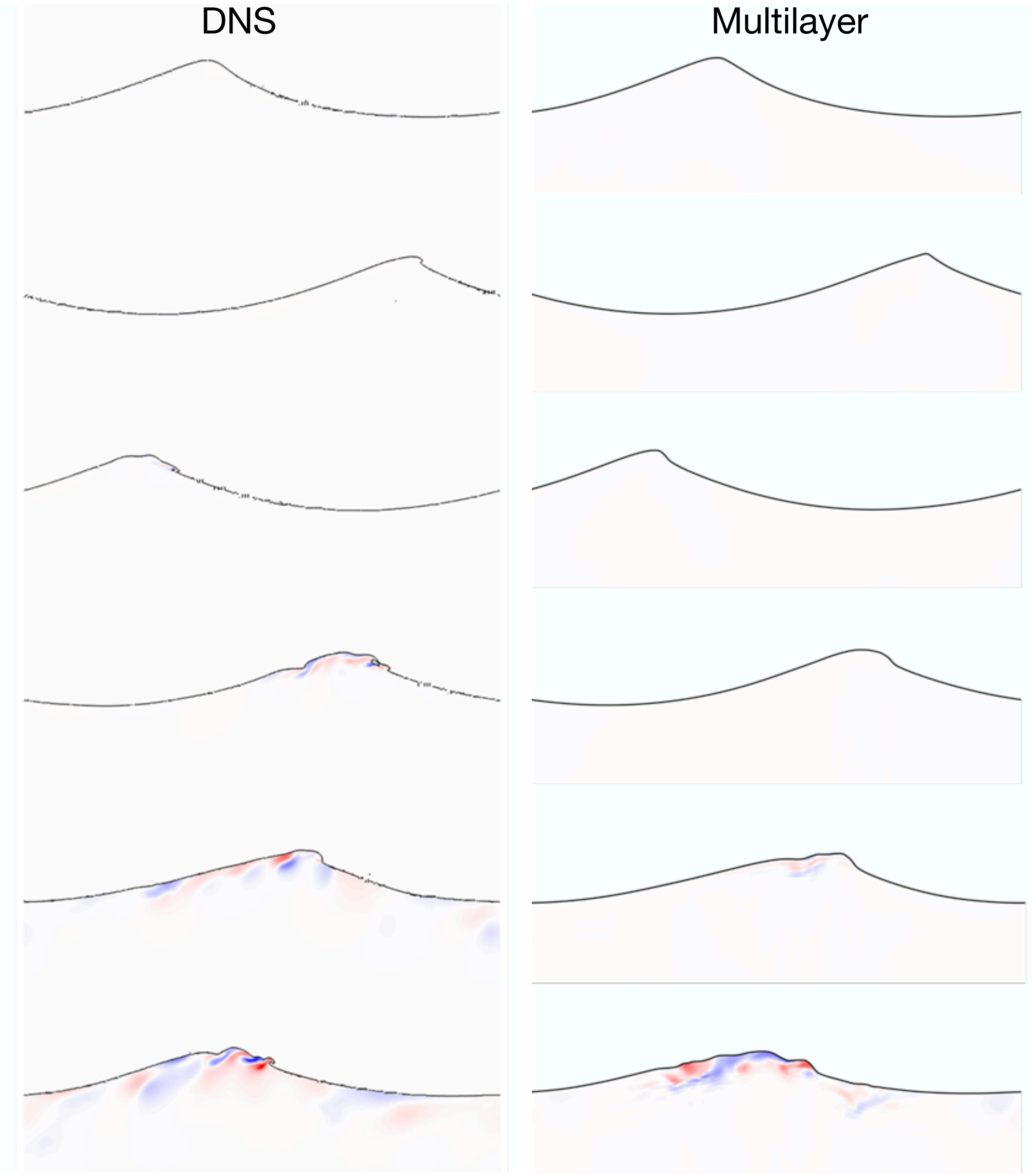

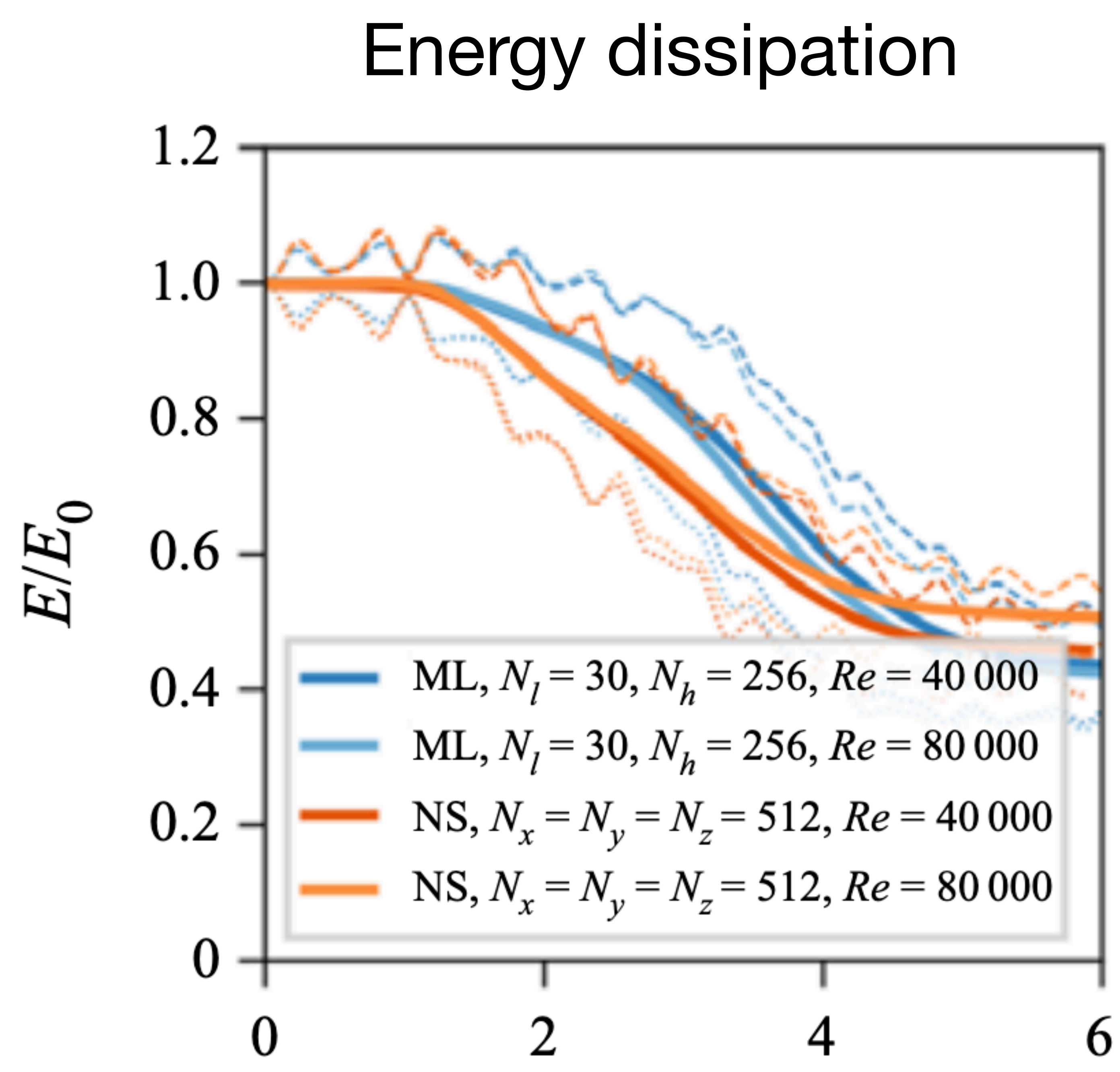

Good agreement with DNS for wave breaking (Wu et al. 2023)

Wind-forcing schemes derivation

Additional wind-forcing scheme is needed for multilayer simulation

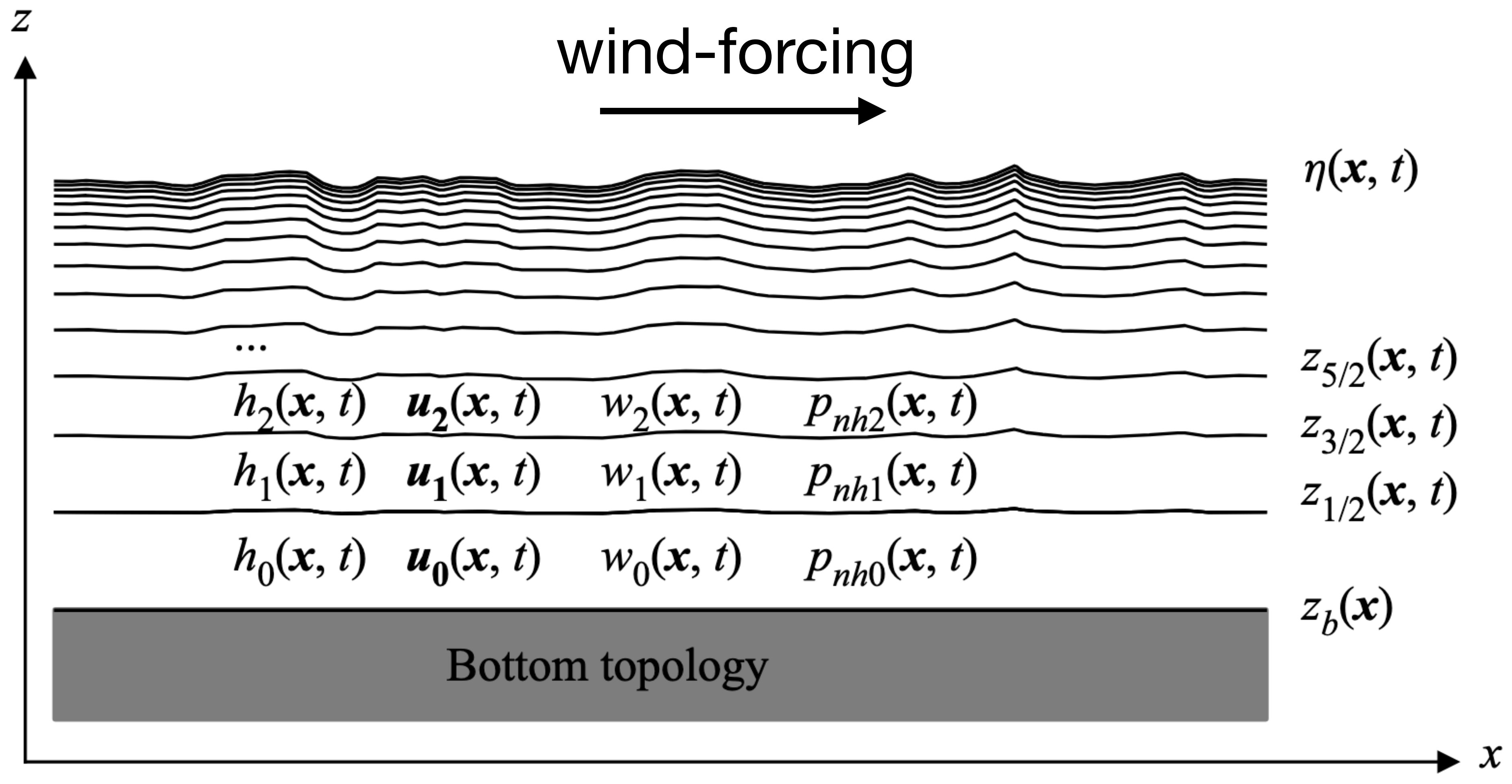

(Wu et al. 2023)

Wave form drag formula

Local wave form drag:

$$F_p(x, y, t) = p_s(x, y, t)\eta_x(x, y, t)$$

Total form drag from Miles' theory:

$$F_p^{Miles} = \frac{1}{2}\beta(ak)^2\tau_0 = \frac{1}{2}\beta(ak)^2\rho_a u_*^2$$ (Miles 1957)

In the multilayer simulation, we assume surface pressure:

$$p_s(x, y, t) = p_0(t)\eta_x(x, y, t)$$

Total form drag from simulation:

$$F_p^{sim} = \langle p_s\eta_x\rangle = \langle p_0\eta_x^2\rangle = \frac{1}{2}p_0(ak)^2$$

↓

p_0 is constant with time, in accordance with Miles' theory

Validations for 2D single-wave

2D decaying wave

$$E = E_0 \exp\left(-4\nu k^2 t\right)$$

(Fedorov & Melville, JFM, 1998)

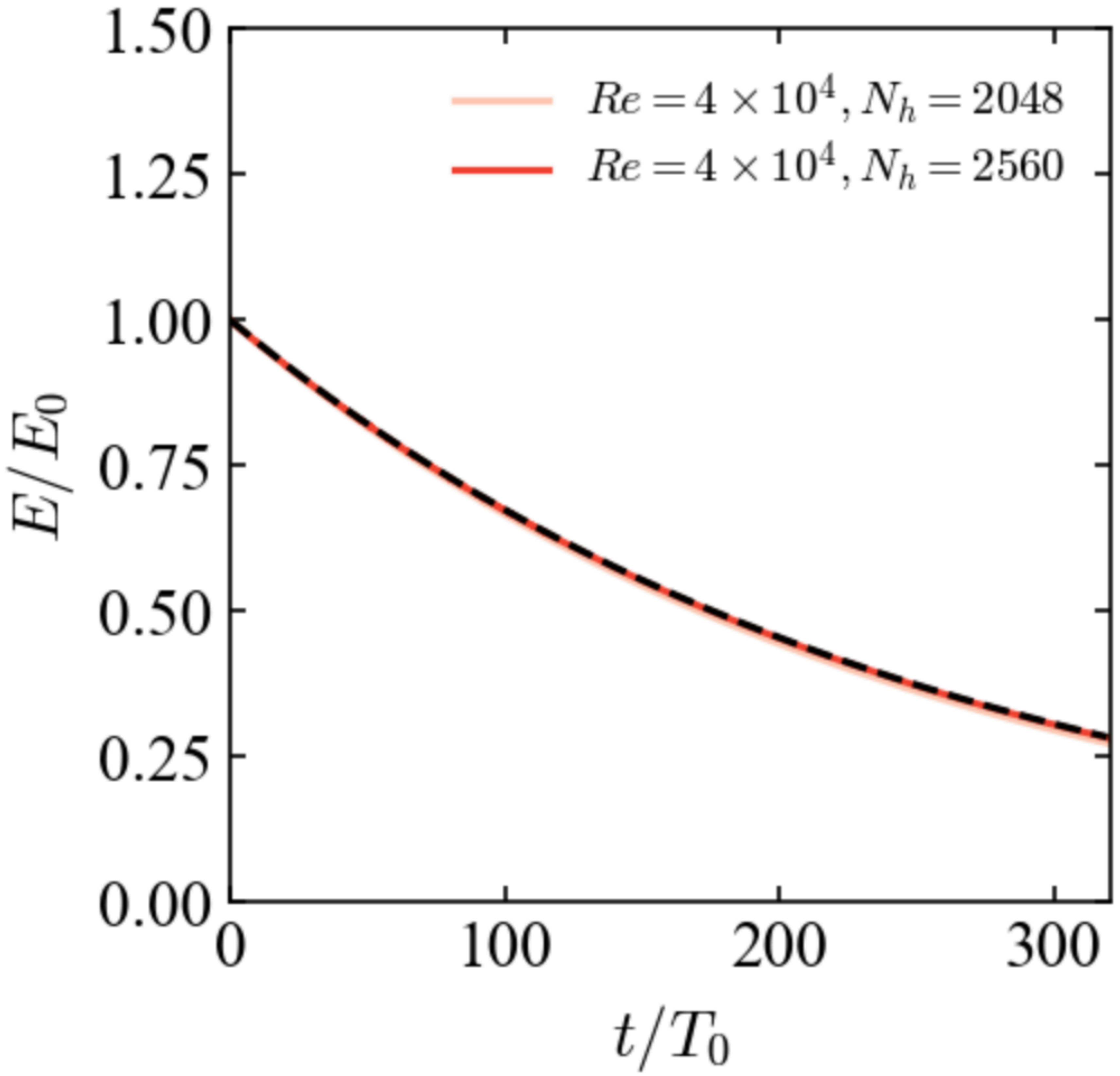

Forced linear wave

$$p_0 = \frac{4\nu a k^2}{c_0},\ \theta = \frac{\pi}{2}$$

(Fedorov & Melville, JFM, 1998)

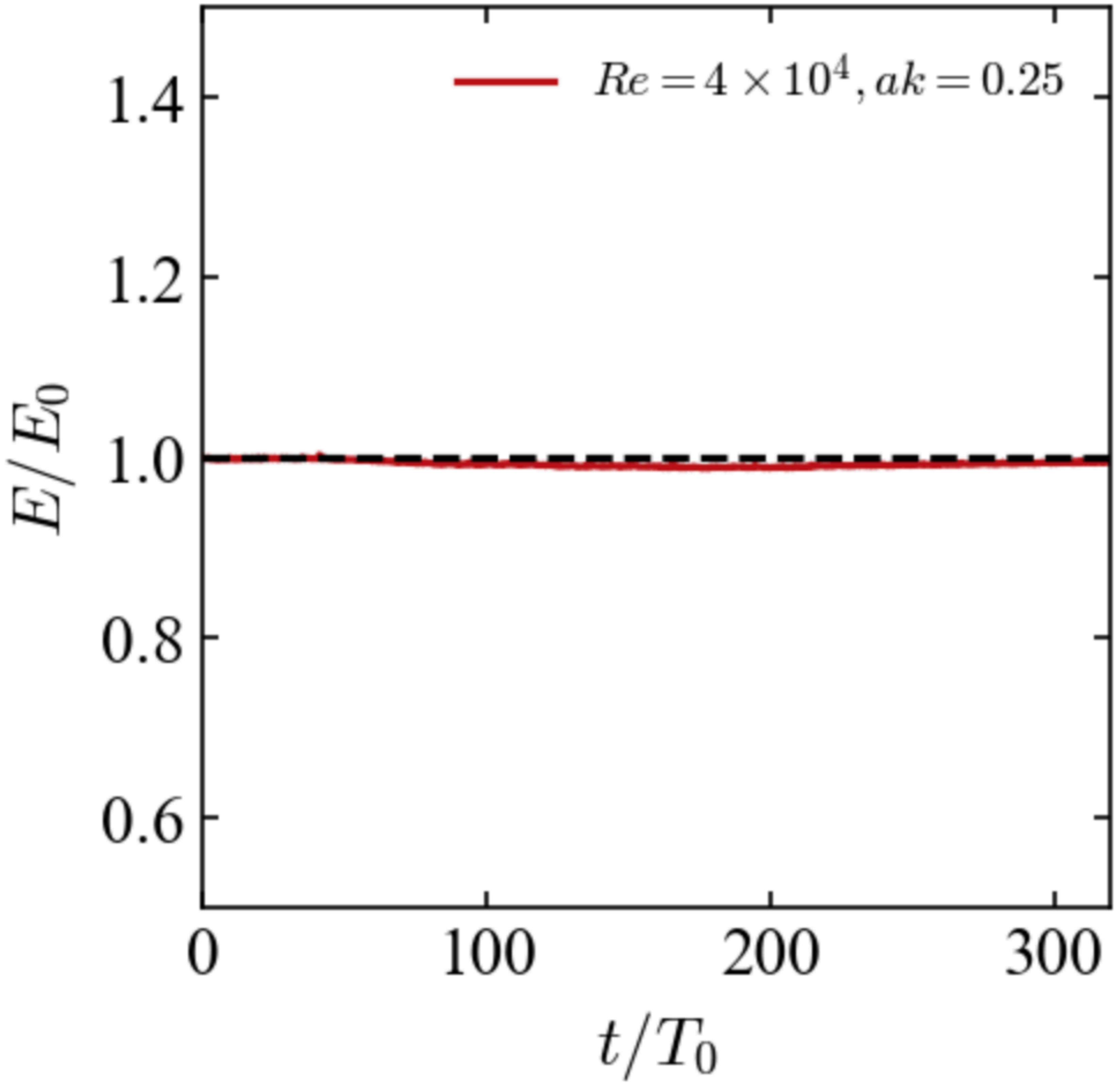

The multilayer simulation results match well with theoretical predictions for forcing.

Simulation setup: wind forcing on a broad-banded wave field

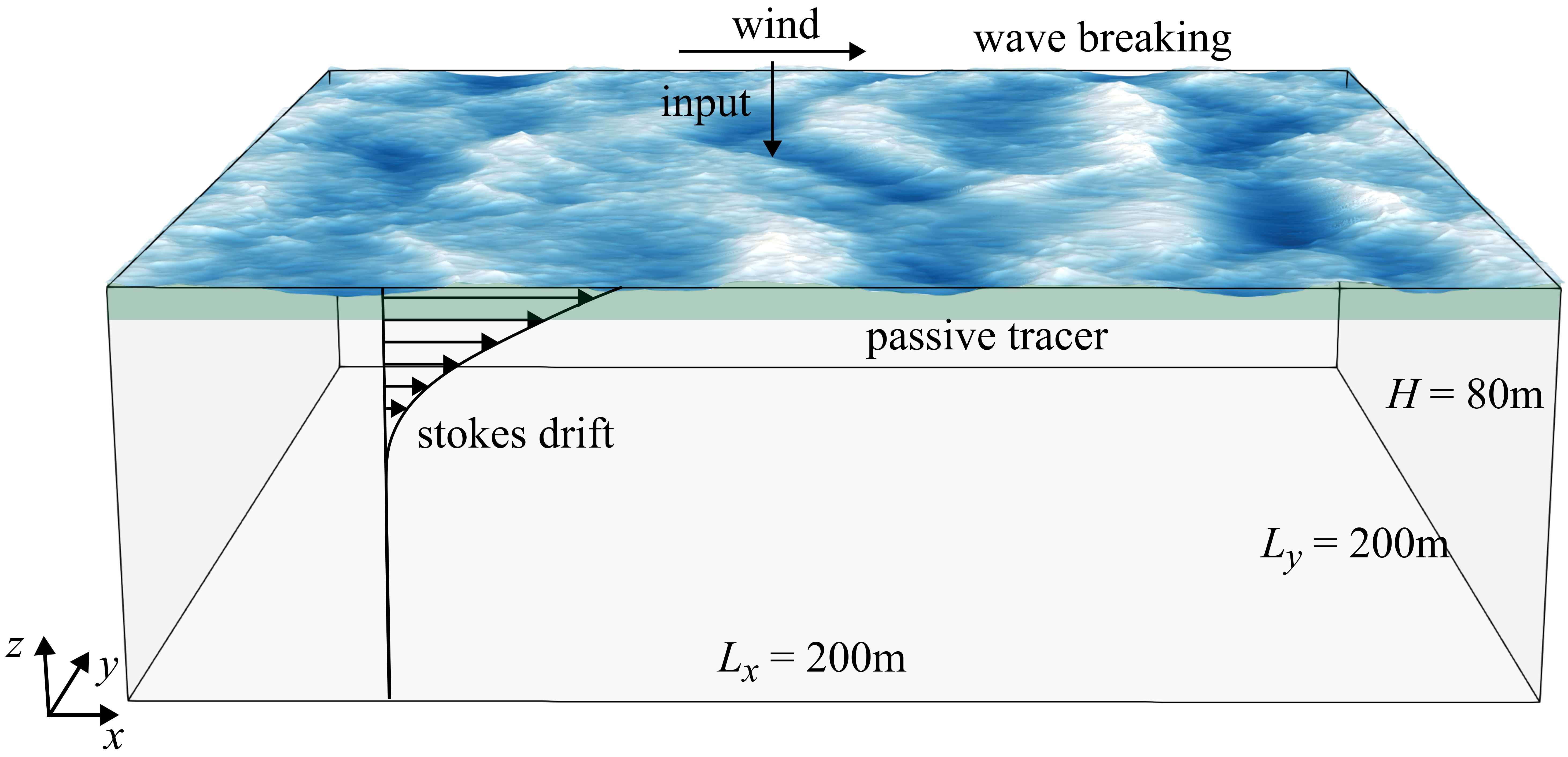

Main control parameters (without forcing):

- Dimensional:

$$k_p,\ H_s,\ \rho,\ \nu,\ g$$

- Dimensionless:

- Wave steepness: $k_p H_s = [0.1 - 0.4]$ (main parameter)
- Reynolds number: $Re = c_p \lambda_p / \nu$

Initial condition:

A typical wind wave energy spectrum (Wu et al. 2023):

$$\phi(k) = P g^{-1/2} k^{-5/2} \exp[-1.25(k_p/k)^2]$$

Upper ocean turbulence under wind-wave breaking

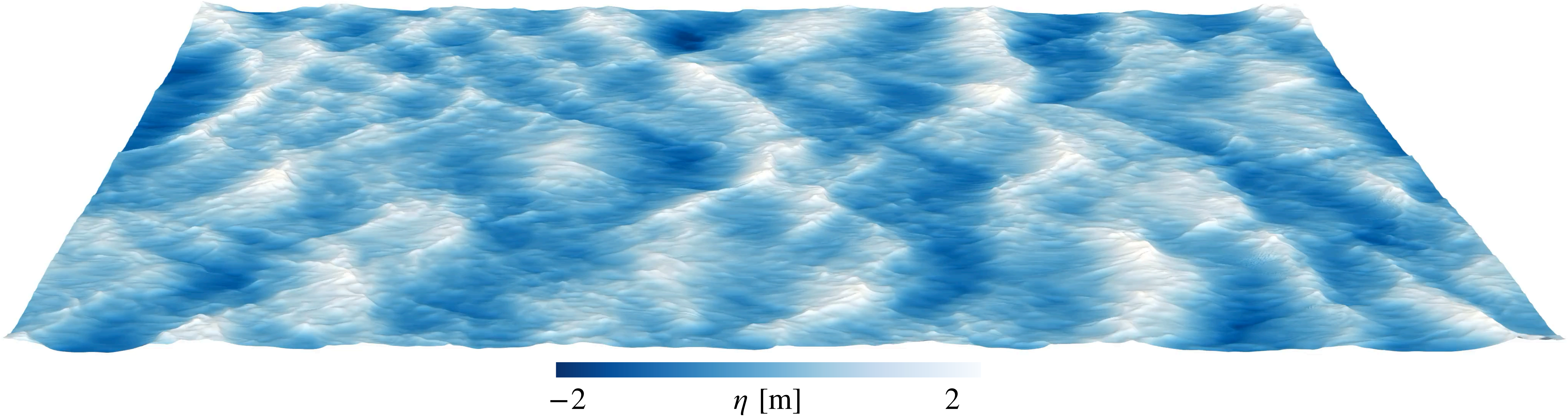

- **Wave statistics?**
- Underwater dissipation?
- Flow and scalar field patterns?

Wind input source term compared to spectral formulation S_{in}

- We calculate the spectral S_{in} from our simulation based on

Real: $S_{in}(x,y) = \frac{1}{\rho_w g} \underbrace{p_s(x,y)\mathbf{n}}_{\text{Normal pressure}} \cdot \underbrace{\mathbf{u_s}}_{\text{Surface velocity}} \approx p_s(x,y) \cdot u_z(x,y)$

Spectral: $\hat{S}_{in}(k,\theta) = \frac{\mathscr{R}(\hat{p}_s \cdot \hat{u}_z^+)}{\rho_w g}$ $\quad \cdot^+$ — complex conjugate

- We compare with the S_{in} model from Janssen (1989, 1991):

$$\hat{S}_{\text{in}}(k,\theta) = \frac{\rho_a}{\rho_w}\beta\left(\frac{u_*}{c}\cos\theta_w\right)^2 \omega F(k,\theta),\ \ \beta = 50$$

also the model from WAMDI group 1988:

$$\hat{S}_{\text{in}}(k,\theta) = 0.25\frac{\rho_a}{\rho_w}\left(\frac{28u_*}{c}\cos\theta - 1\right)\omega F(k,\theta)$$

Forcing parameters

u_* [m/s]	c_p/u_*	U_s [m/s]	La
0.84	9.4	0.02–0.16	0.42–1.20
1.9	4.2	0.02–0.4	0.40–1.80
1.92	4.1	0.19–0.41	0.40–0.59
1.92	4.1	0.13–0.38	0.40–0.71

u_* - from $S_{in}(k)$ J89 model fit

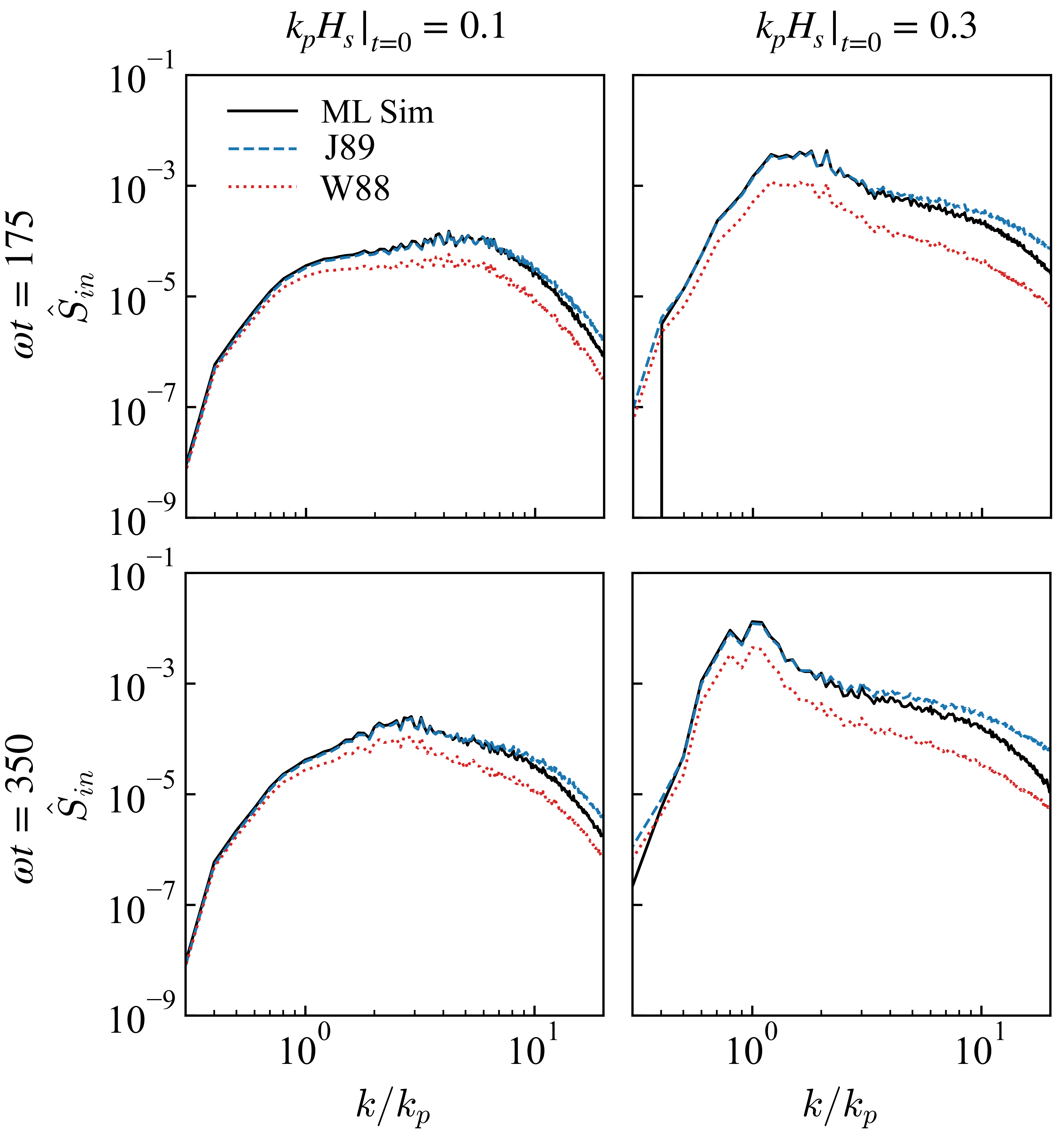

Evolution of wave statistics

Effective fetch: $X = U_{10}(t + t_0)$ Nondimensional energy: $\varepsilon_* = \dfrac{g^2 H_s^2}{16 u_*^4}$

Nondimensional fetch: $X_* = \dfrac{gX}{u_*^2}$ Nondimensional peak frequency: $\nu_* = \dfrac{u_*}{T_p g}$

$$\phi(k) = \int F(k,\theta) k d\theta, \; F(k,\theta) = \hat{\eta} \cdot \hat{\eta}^+ = |\hat{\eta}|^2$$

Time evolution of wave spectrum $\phi(k)$

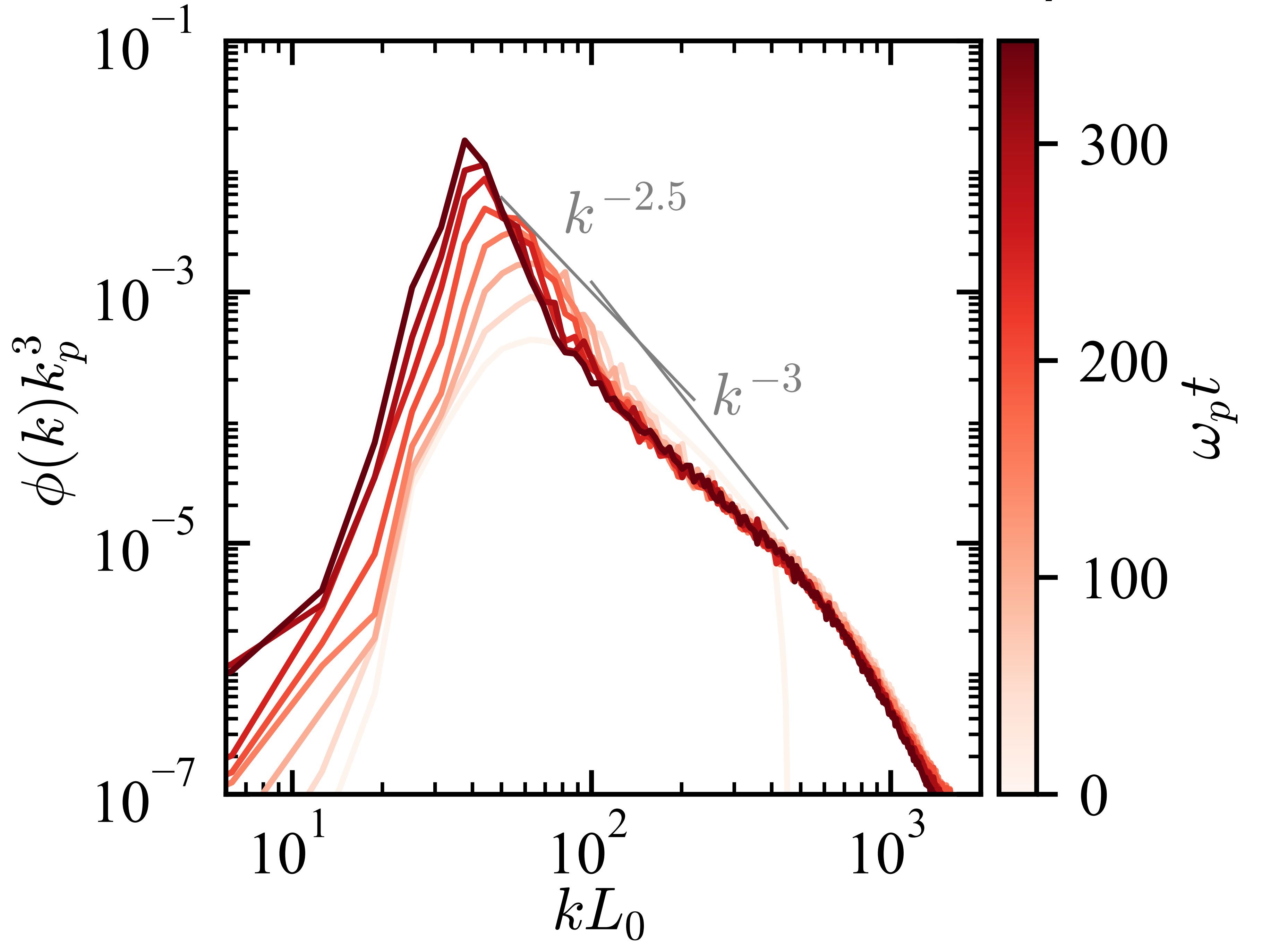

Nondimensional fetch limited relationships

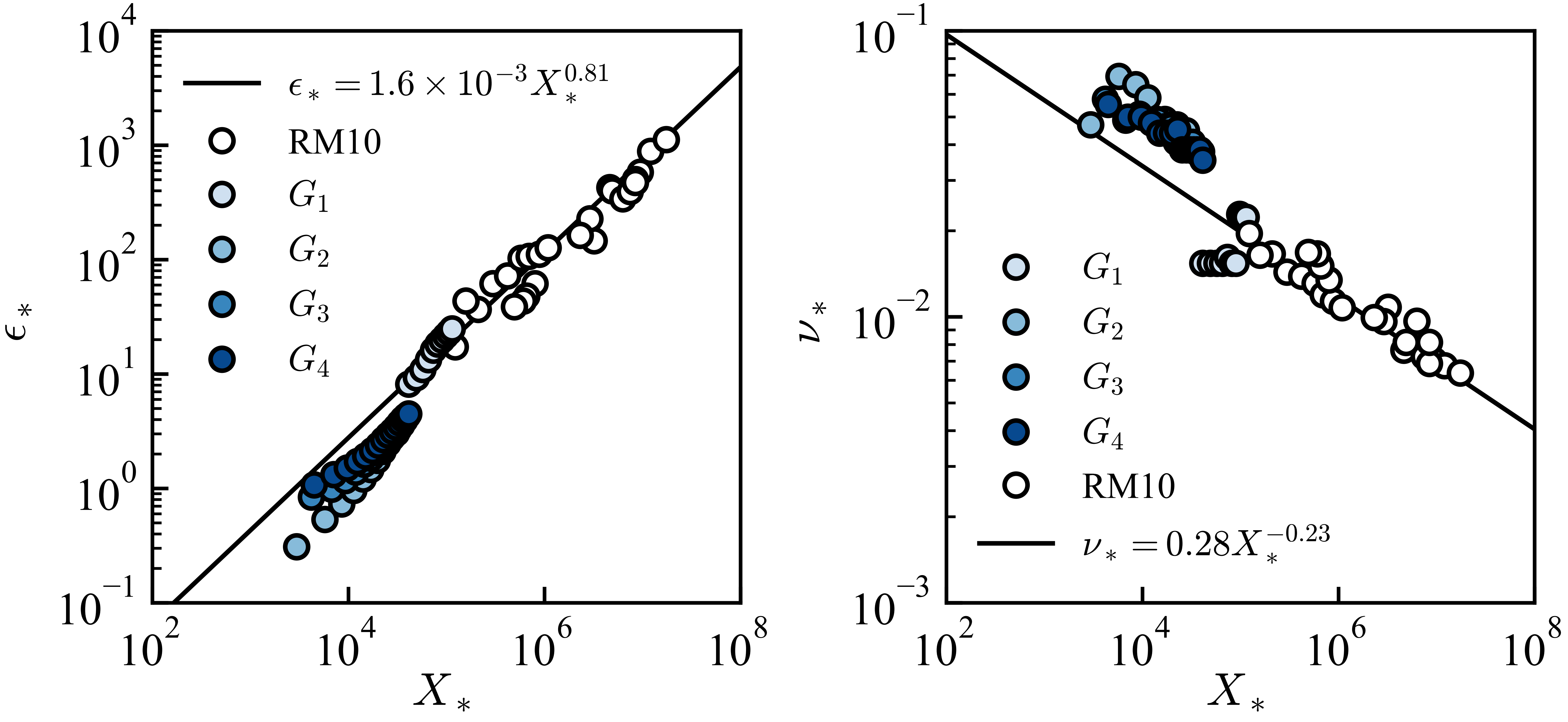

- Saturation: k^{-3} spectral shape.
- As time evolves, the wave grows and k_p decreases
- Multilayer simulation results follow the fetch-limited relationships from reference data from Romero & Melville, 2010

Breaking distribution

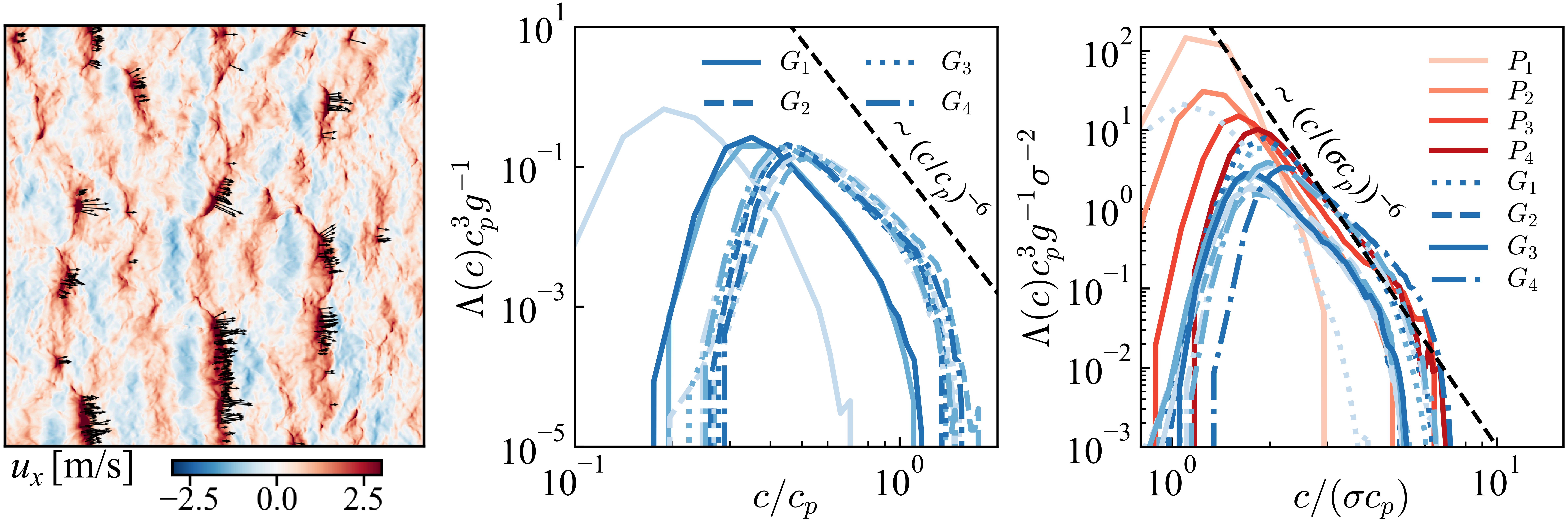

- $\Lambda(c)$ - The breaking front length at the local wave speed c, captured by the local wave curvature.
- $\Lambda(c)$ distribution depends on the wind-wave condition, while the $\Lambda(c) \sim c^{-6}$ scaling always exists and follows Phillips' theoretical prediction.
- $\Lambda(c)$ rescaled by the r.m.s. slope σ collapse the distributions under different wind-wave conditions (Wu et al. 2023).

Upper ocean turbulence under wind-wave breaking

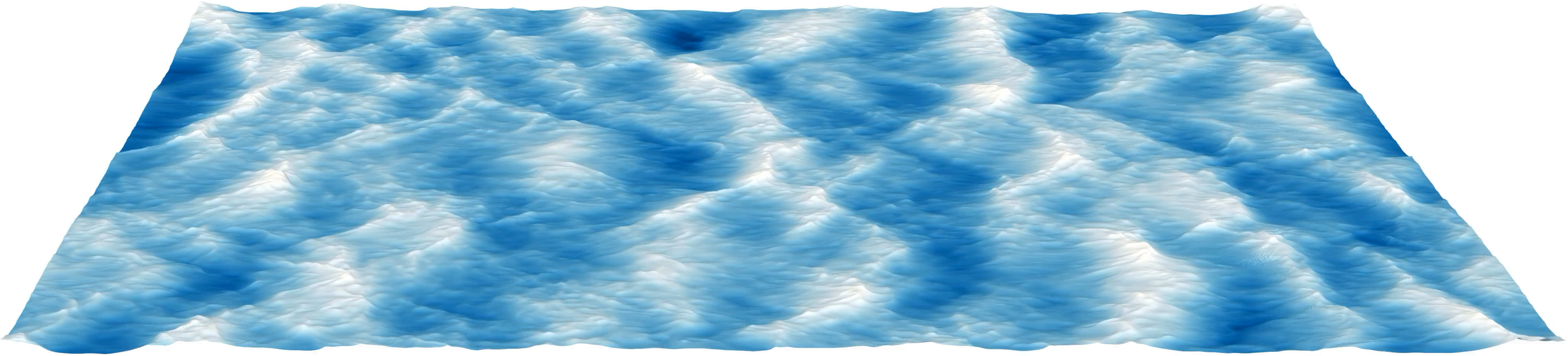

- Wave statistics?
- **Underwater dissipation?**
- Flow and scalar field patterns?

Dissipation profiles

- The dissipation profiles calculated by $\varepsilon(z) = \nu\langle s_{ij}s_{ij}\rangle$
- The near-surface dissipation (above -2m) profile reach a steady state, while deeper water dissipation keeps increasing as the wave-breaking induced turbulence keeps penetrating into deeper water as time evolves.

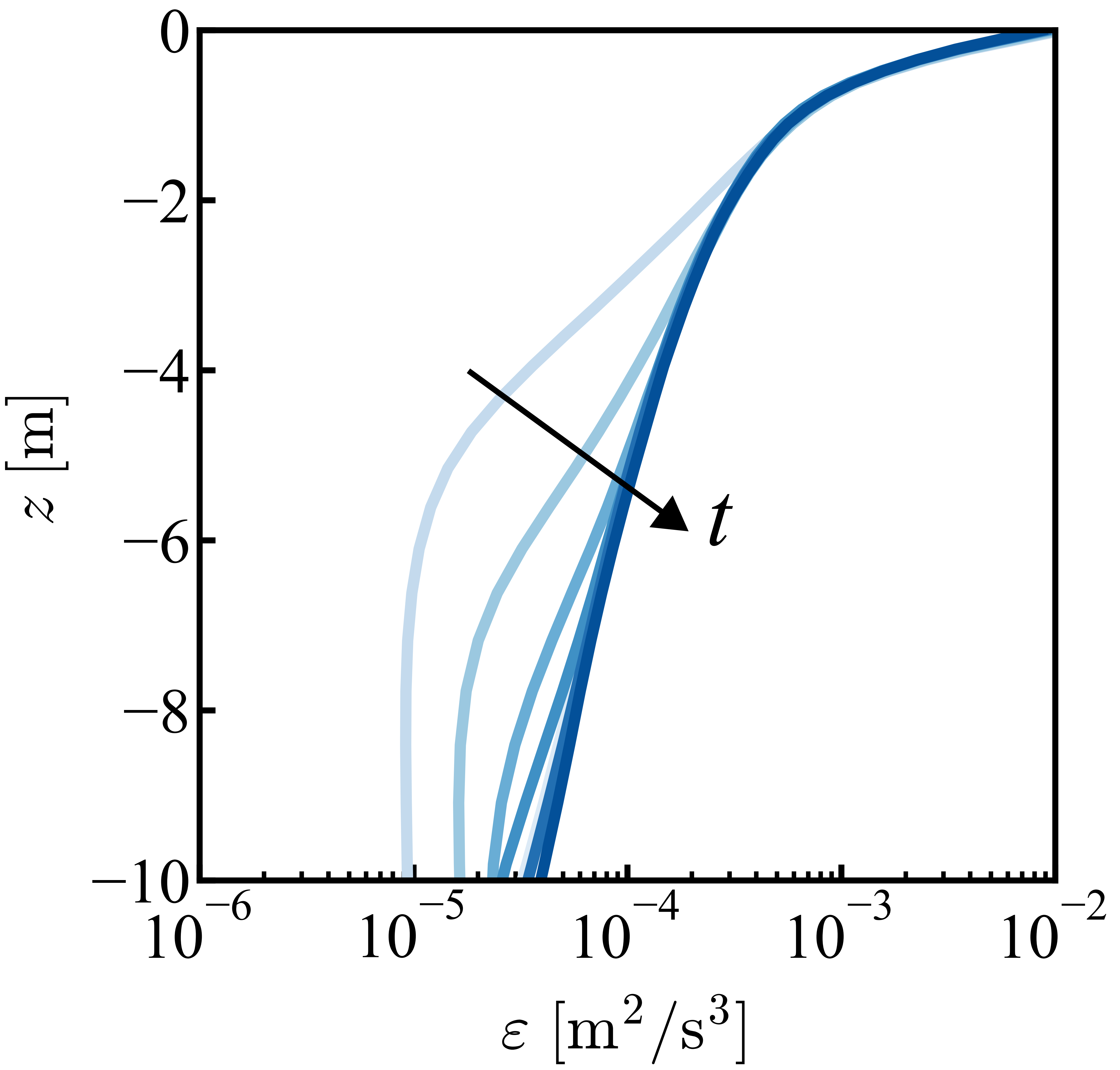

Normalized dissipation profiles

$$F_{in} = \rho_w g \int S_{in}(k,\theta) k dk d\theta$$

Dissipation profile normalized by Φ

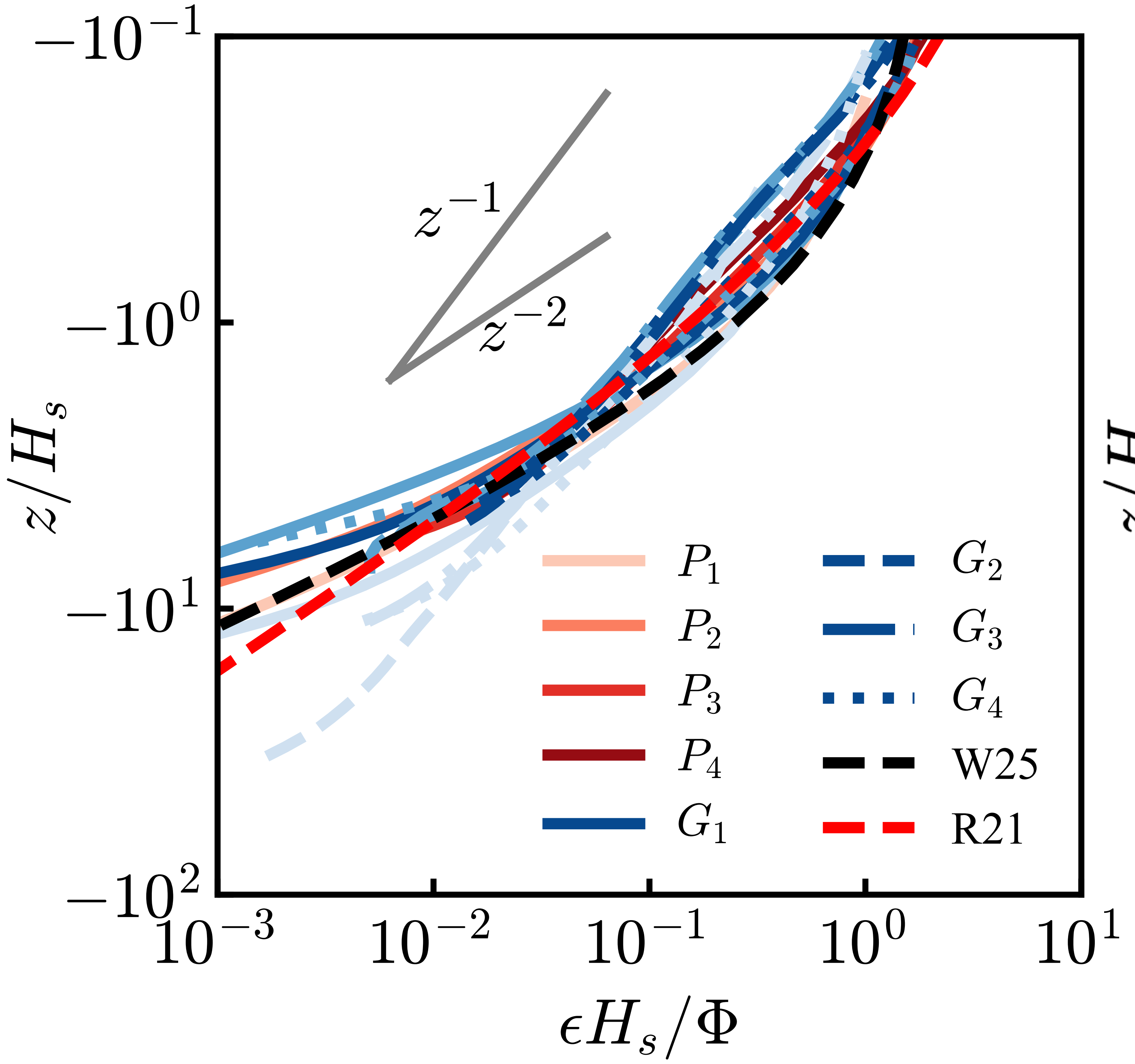

Φ - depth-integrated dissipation

Dissipation profile normalized by wind energy input F_{in}

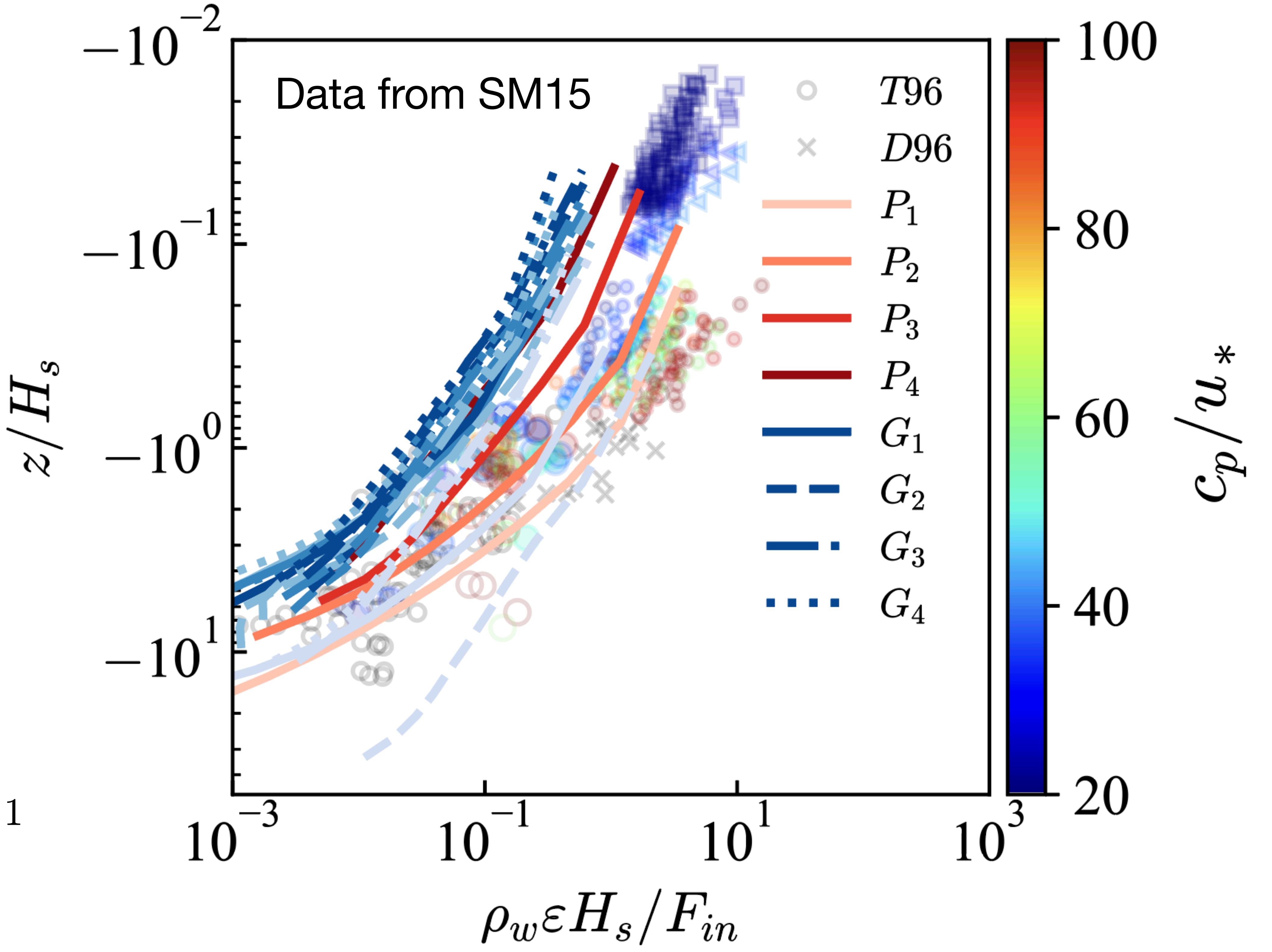

- We normalize the dissipation profiles in two different ways.
- The normalized dissipation profiles by the depth-integrated dissipation rate show a good collapse and the model predictions (Wu et al. 2025; Romero 2021).
- The normalized dissipation profiles by F_{in} shows a dependence on c_p/u_*, in agreement with the data from Sutherland & Melville 2015.

Dissipation & F_{in}, F_{ds}

$$F_{ds} = \rho_w g^{-1} \int bc^5 \Lambda(c) dc \quad \begin{cases} F_{ds1}: b(k) = A(B(k)^{1/2} - B_T^{1/2})^{5/2} \\ F_{ds2}: b = 0.01 \end{cases}$$

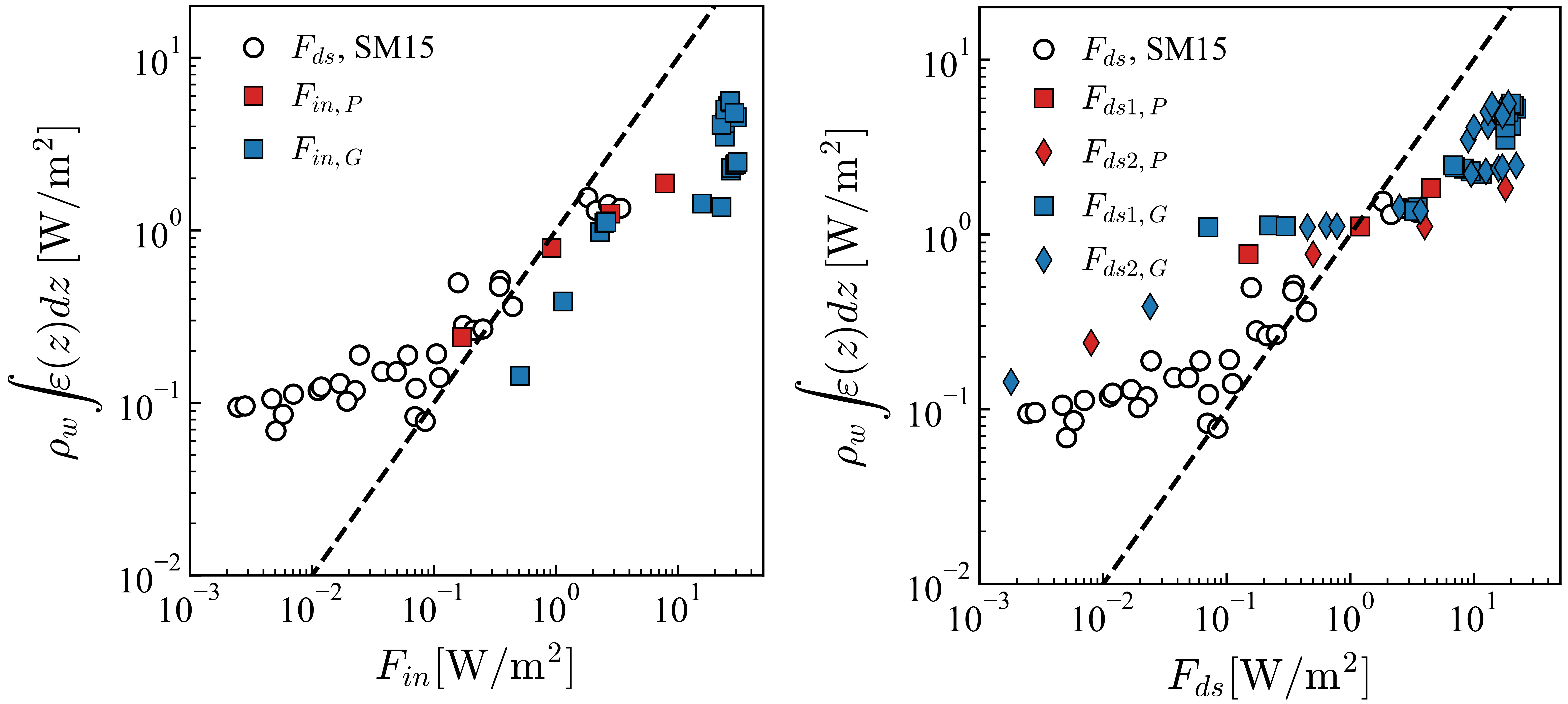

- The total dissipation and F_{in} from the multilayer simulation agrees with field data
- F_{ds} is the dissipation from wave breaking.
- F_{ds} from simulation depends on the estimation of the breaking parameter b, especially at low $k_p H_s$

Upper ocean turbulence under wind-wave breaking

We add passive tracer initially at $z > -1.3\mathrm{m}$

- Wave statistics?
- Underwater dissipation?
- **Flow and scalar field patterns?**

Scalar field evolution

The scalar field at the initial interface for the growing case

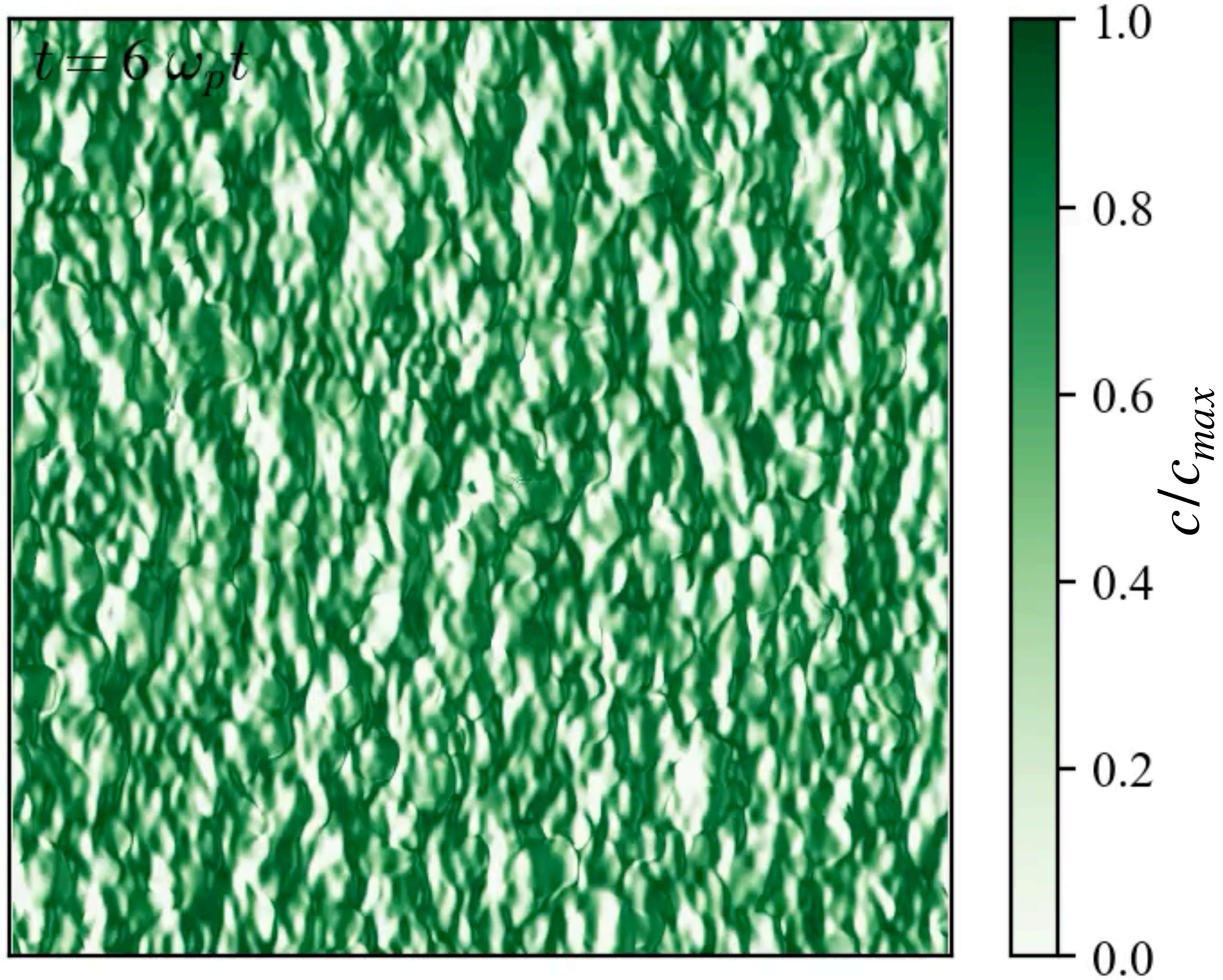

Wind

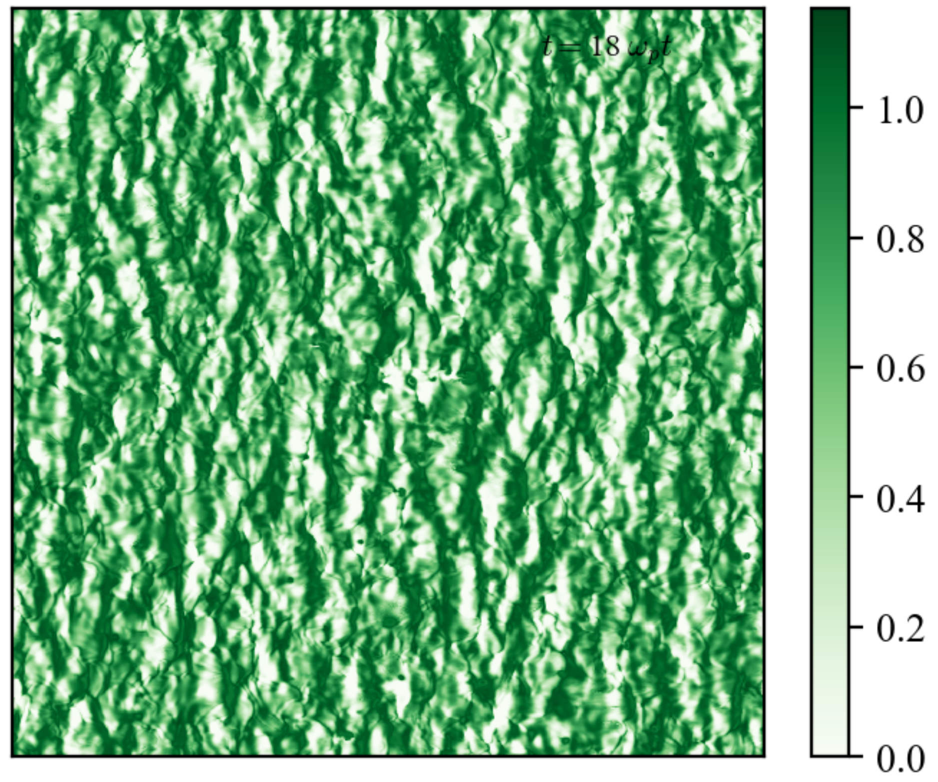

- At the very beginning ($\omega_p t \approx 10$)
- spanwise wave pattern following the surface wave shape

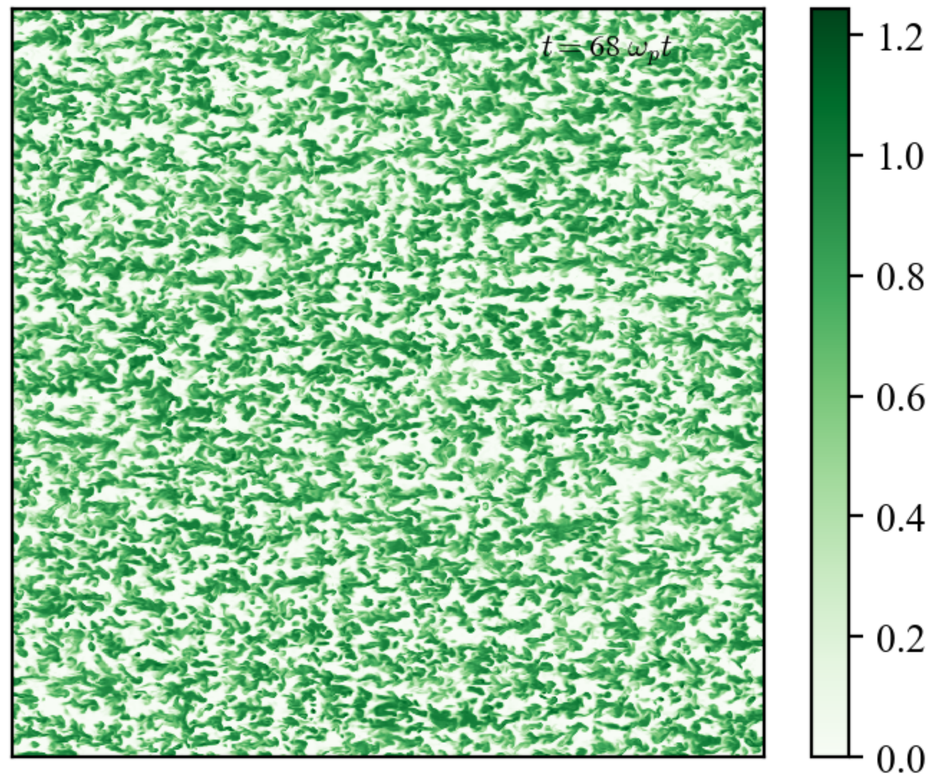

- At the early stage ($\omega_p t \approx 60$)
- Small-scale streamwise streak pattern starts to dominate

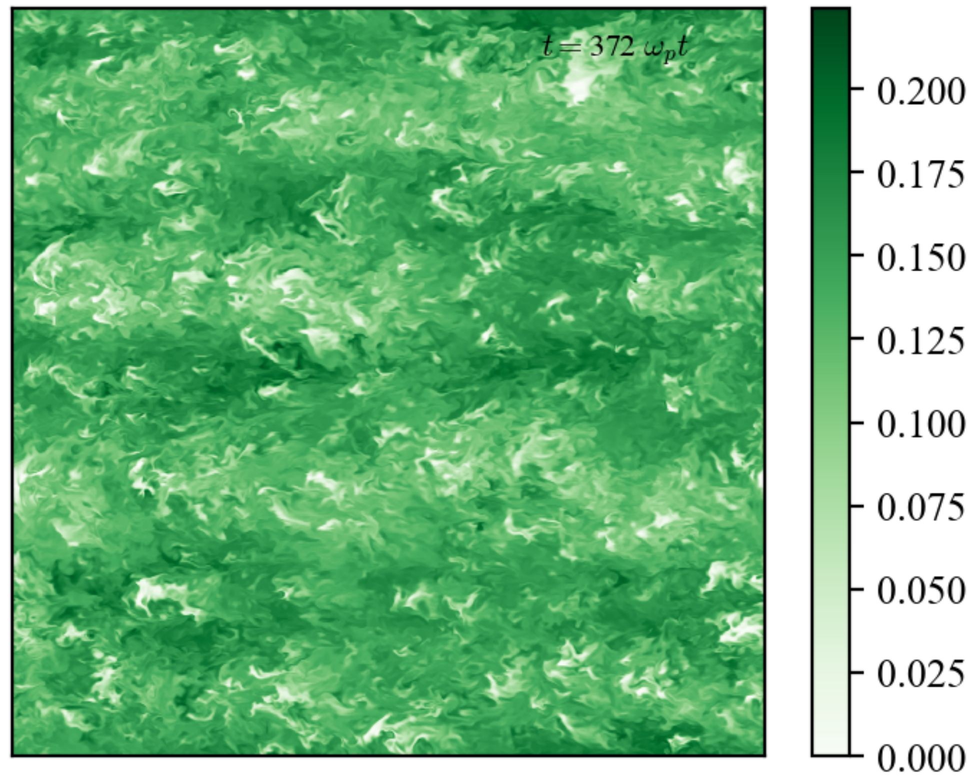

- At the later stage ($\omega_p t \approx 370$)
- Langmuir circulation pattern dominates

c profile evolution

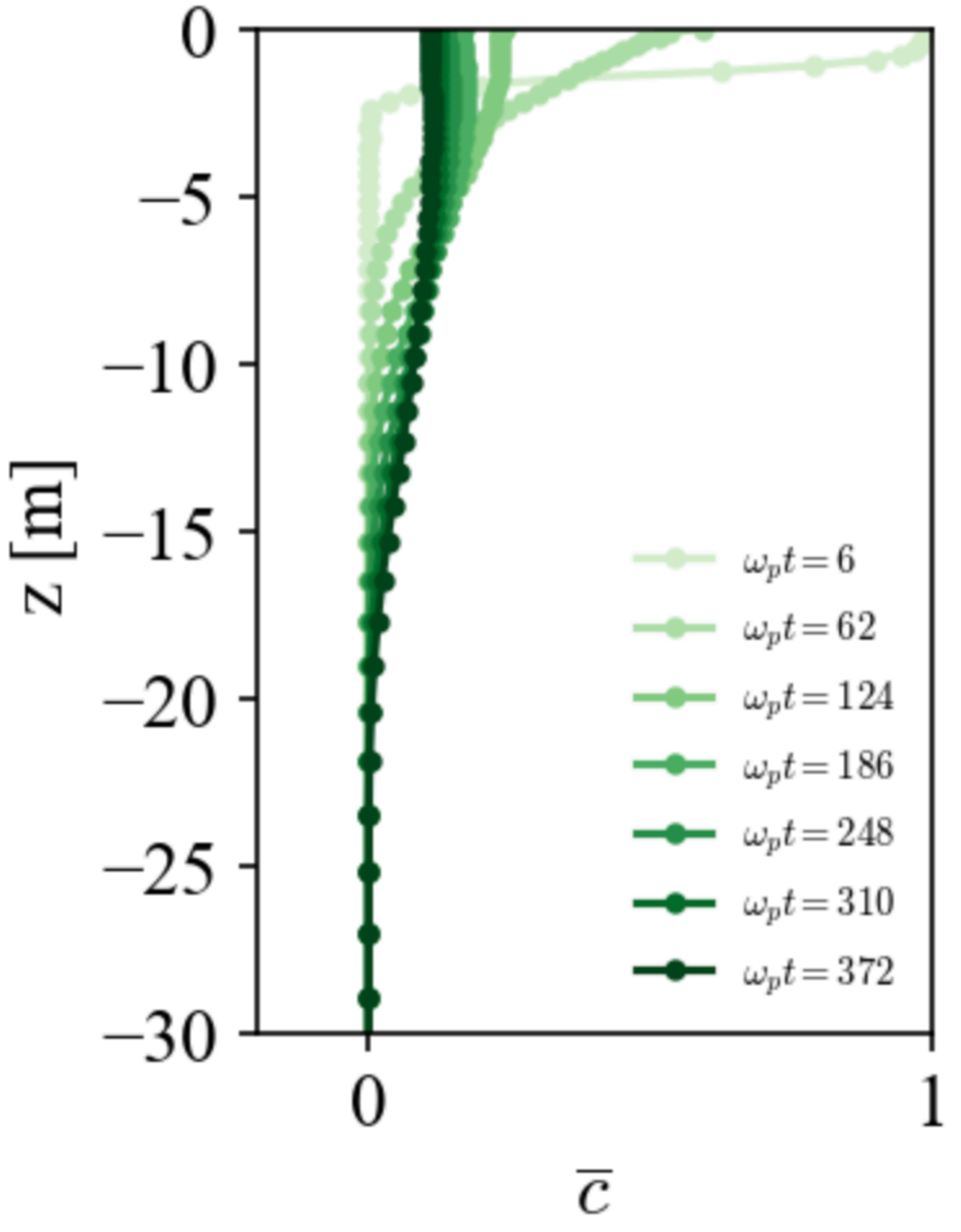

Langmuir circulation pattern

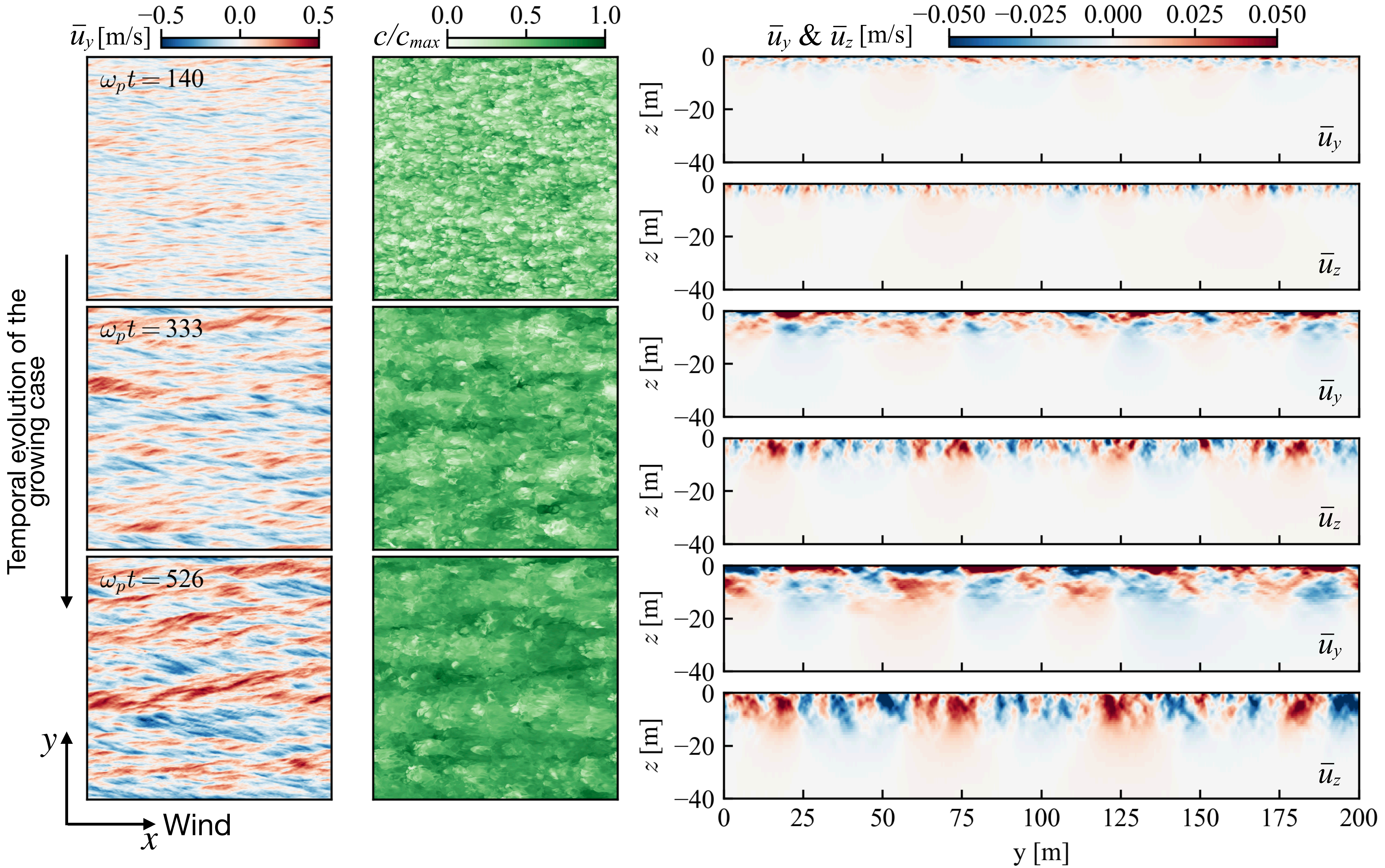

As time evolves, the velocity magnitude and the typical length scale increases, and the velocity penetrates deeper.

Evolution of LC - velocity scale

- u_y is averaged within one wave period
- Stokes drift is calculated by $U_s = 2g^{1/2}\int k^{3/2}\phi(k)dk$

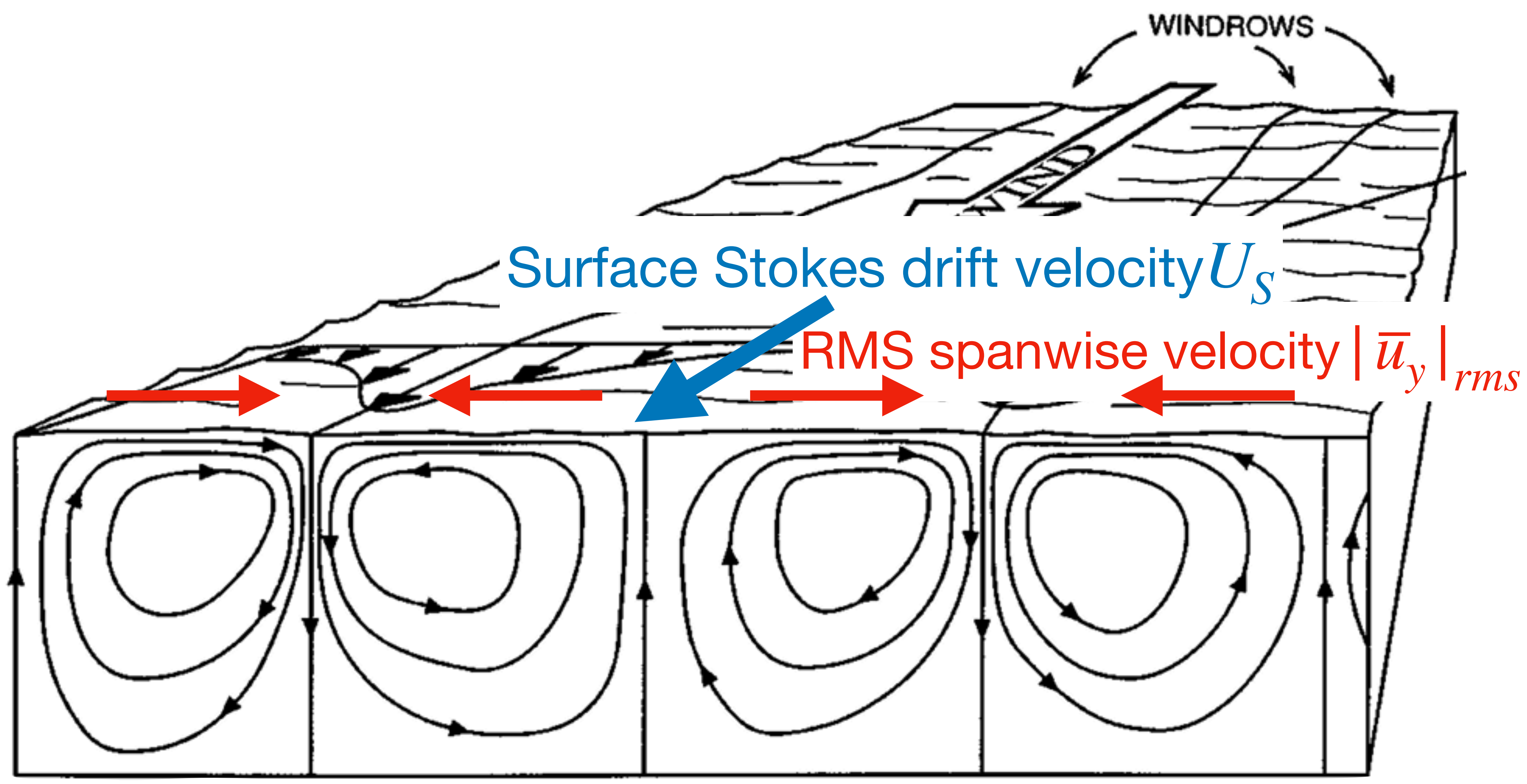

(Thorpe 2004)

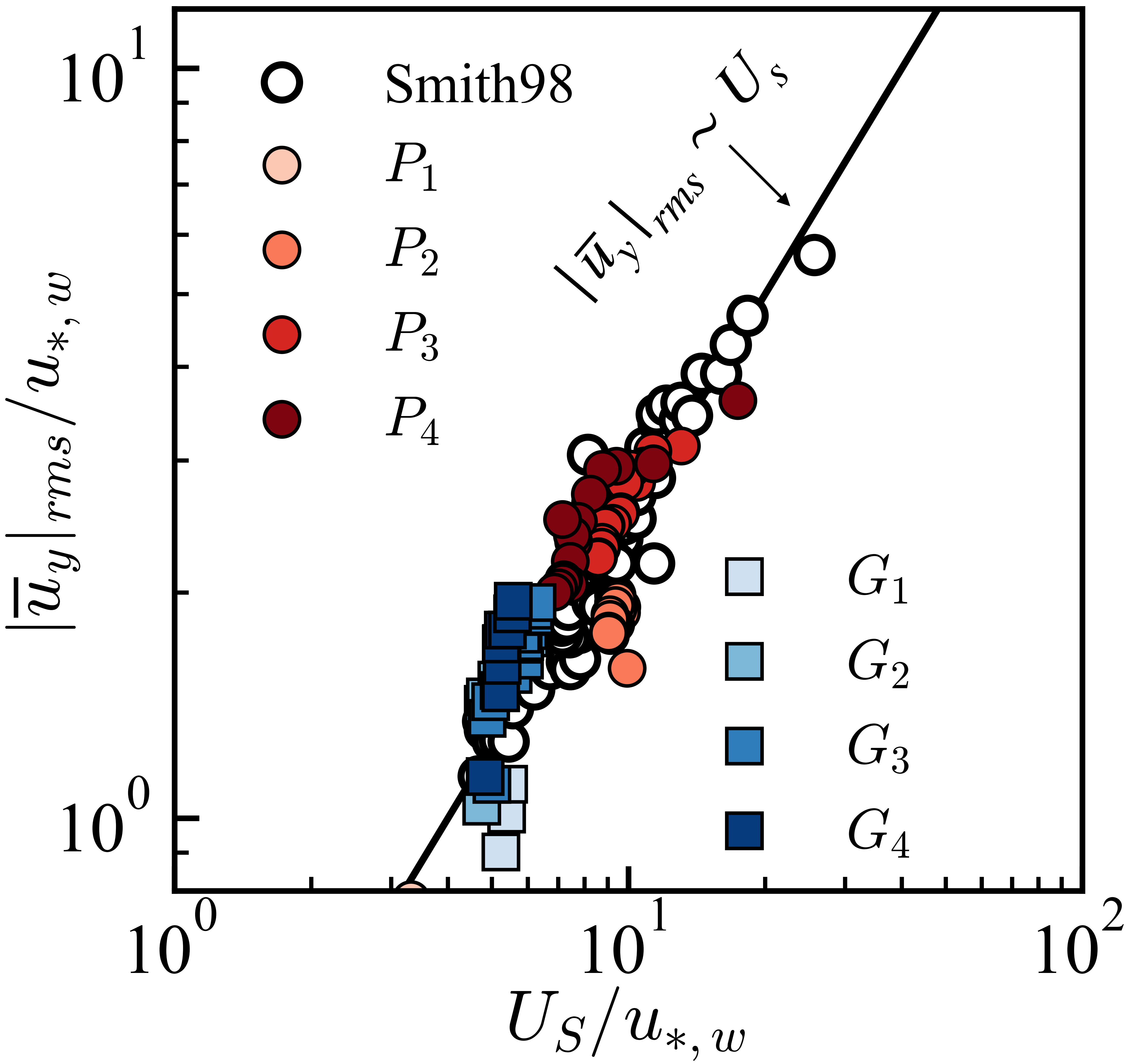

- The velocity statistics follows the field data.

Craik–Leibovich (CL) mechanism for Langmuir circulation

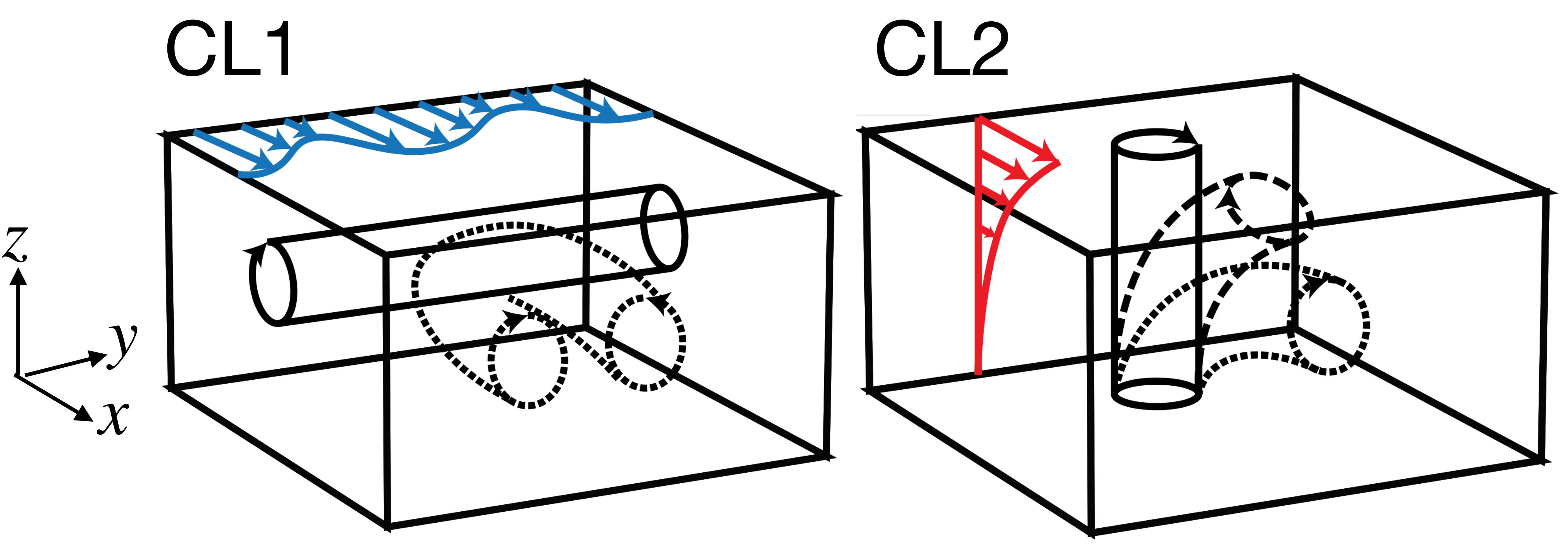

Lateral variation of flow distort the vortex

Vertical stokes drift distort the vortex

CL1: Horizontal tilting term: $T_h = \omega_y \frac{\partial \overline{u_x}}{\partial y}$

CL2: Vertical tilting term: $T_v = \omega_z \frac{\partial \overline{u_x}}{\partial z}$

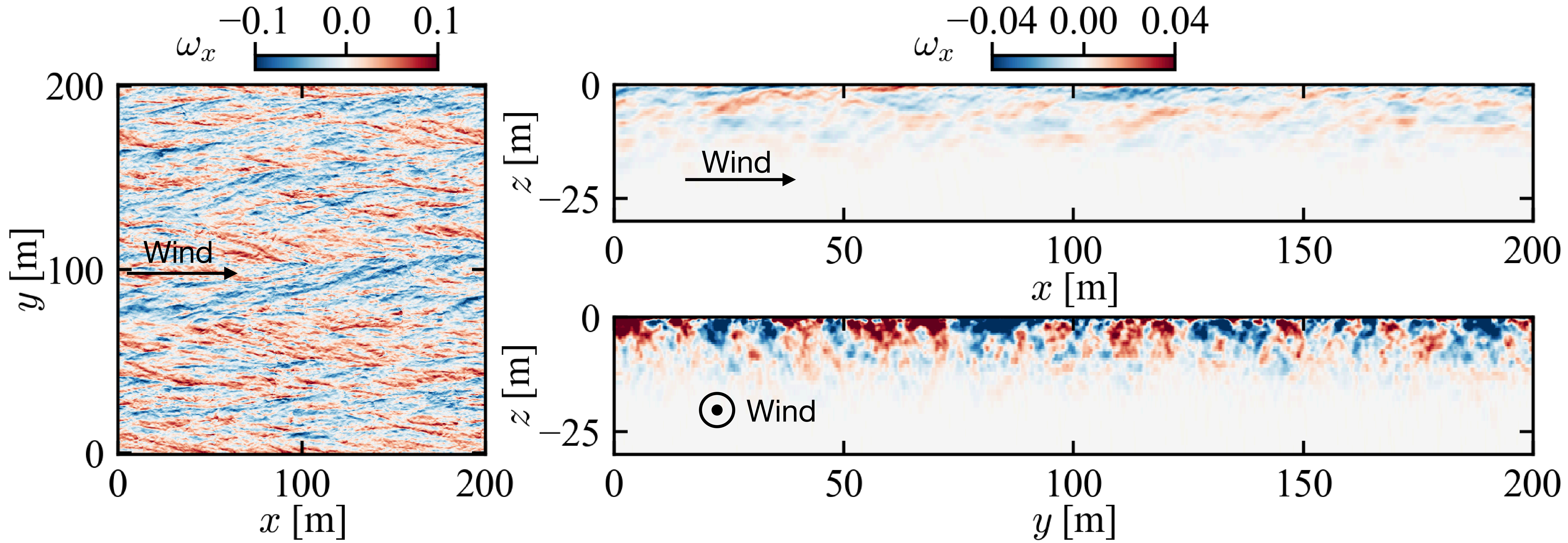

Craik–Leibovich (CL) mechanism for Langmuir circulation

The cross-spectrums show the contribution of the tilting terms to ω_x at different k

- CL2 dominates the vorticity tilting through the k-regime
- CL1 contributes to the low-k regime

The spatial distribution of Stokes drift could be important in the large-scale LC pattern, consistent with the findings from recent studies (Fujiwara & Yoshikawa 2020; Scully & Zippel 2024)

Cross-spectrum: $C(\omega_x, T_v)$ & $C(\omega_x, T_h)$

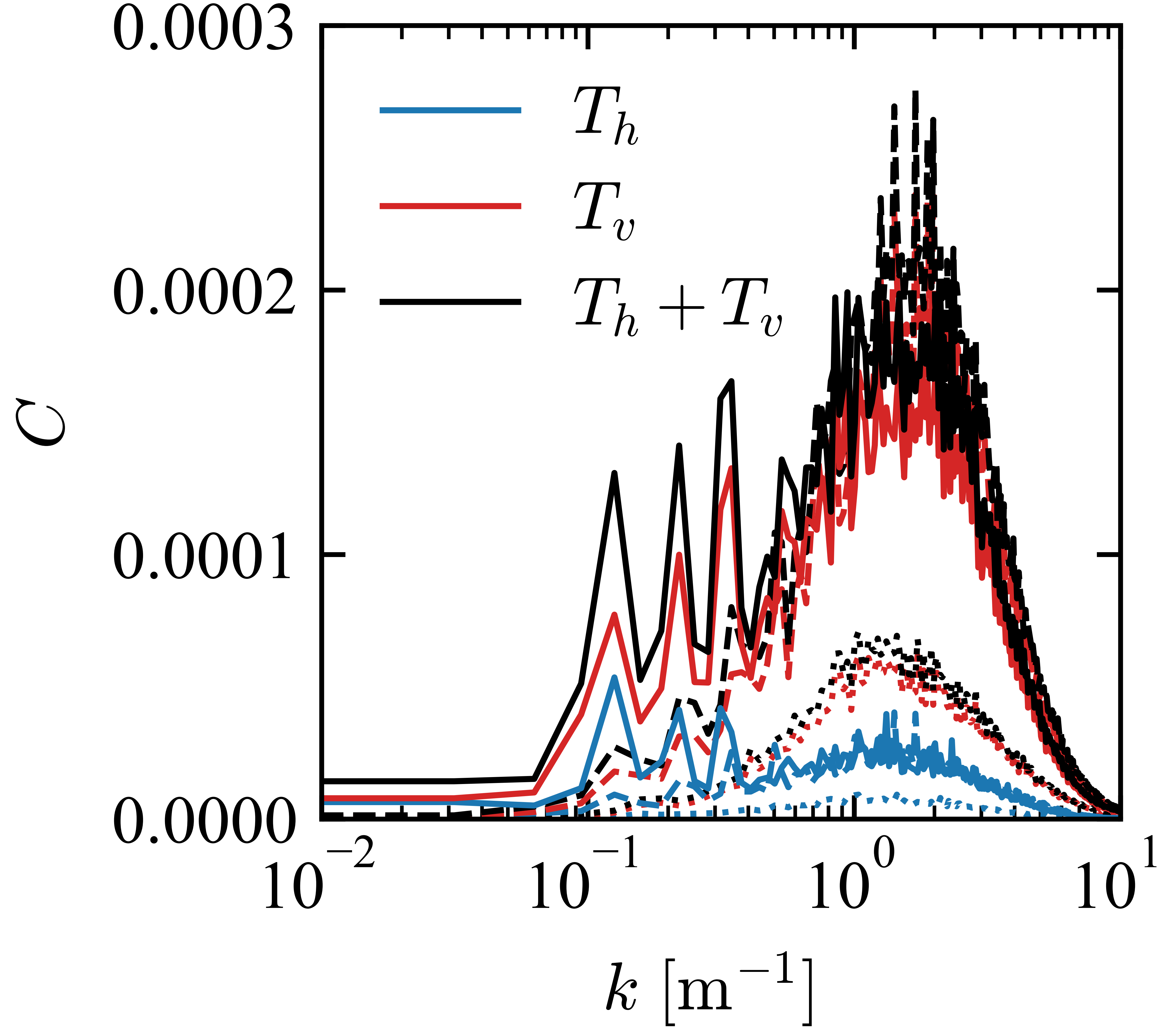

Conclusion

- We proposed two forcing schemes for the multilayer simulation of the **wind-forced broadband wave field**.
- We quantitatively compared the **wave statistics, wave breaking statistics, S_{in} & S_{ds}, underwater dissipation profile, and scalings** with references data, which all show reasonable agreements.
- We observed the evolution of the scalar field pattern from a **wave-like pattern** to a **small-scale streak pattern** to a **large-scale Langmuir pattern**. We also quantitatively analyzed the spacing, velocity strength, and vorticity.

Thanks!

High Meadows Environmental Institute

NASA

NSF

PRINCETON UNIVERSITY